

© 2006 by Alan M. Bolind. All rights reserved.

CONTROL OF THE OXYGEN CONTENT OF THE COVER GAS IN A MOLTEN
LEAD-BISMUTH EUTECTIC SYSTEM

BY

ALAN M. BOLIND

B.S., Webb Institute, 1998

M.S., Webb Institute, 1999

THESIS

Submitted in partial fulfillment of the requirements
for the degree of Master of Science in Nuclear Engineering
in the Graduate College of the
University of Illinois at Urbana-Champaign, 2006

Urbana, Illinois

Abstract

CONTROL OF THE OXYGEN CONTENT OF THE COVER GAS IN A MOLTEN LEAD-BISMUTH EUTECTIC SYSTEM

Alan Michael Bolind
Nuclear, Plasma, and Radiological Engineering Department
University of Illinois at Urbana-Champaign, 2006
James, F. Stubbins, Advisor

This thesis addresses some of the concerns associated with controlling the oxygen content of the environment of a lead-bismuth eutectic (LBE) system. LBE is being considered both as a target material for an accelerator-driven spallation neutron source and as a coolant in a fast reactor. However, LBE (and lead alloys, in general) can cause significant dissolution corrosion of steel system components (such as piping) if the corrosion is not mitigated by the formation of protective oxide layers on the steel surfaces in contact with the LBE. The formation and preservation of the protective oxide layers depends on the oxygen content of the LBE environment. One typical way to control the oxygen content of the LBE environment is to control the oxygen content of the gas covering a free surface of the LBE (that is, the cover gas).

This thesis describes how to control the oxygen content of a cover gas. It begins with a treatment of the thermodynamics of oxide formation, to determine the target oxygen partial pressures necessary for proper protective oxide formation. Next, some methods for verifying the oxygen content of the cover gas, using oxygen sensors, are discussed. Third, various methods for controlling the oxygen content are evaluated, leading to the conclusion that the gas dynamic equilibrium method is the best method. Practical

concerns of this method are then explored, especially concerns about the kinetics of the gas-phase reactions, the dilution and mixing of gases, and the swamping of impurities and leaks.

Acknowledgements

I would like to acknowledge and thank the various individuals and organizations who have had a part in the work that went into this thesis:

- Professor James F. Stubbins, my advisor
- Professor Barclay G. Jones, the second reader of this thesis
- Professor Nick G. Glumac, who provided guidance and software for modeling gas-phase chemical kinetics
- Dr. Ning Li, one of my mentors during my internship at Los Alamos National Laboratory during the summer of 2001. Dr. Li also was instrumental in the formulation of my research program and in the provision of research funds.
- Dr. R. Scott Lillard, my mentor during my internship at Los Alamos National Laboratory during the summer of 2005
- Dr. Eric P. Loewen, who provided guidance in the setup of LBE corrosion experiments
- Dr. Timothy W. Darling, one of my mentors during my internship at Los Alamos National Laboratory during the summer of 2001
- Ms. Cathy Dixon, University Fellowship Program Manager for the University Research Alliance. Ms. Dixon was the key administrator of the fellowship I received for my first two years of graduate school. This fellowship connected me with the Los Alamos National Laboratory.
- The Institute of Nuclear Power Operations, which also provided a one-year fellowship

Table of Contents

List of Figures	viii
List of Tables	ix
List of Symbols	x
1. Introduction	1
2. The Thermodynamics of Oxide Formation	3
2.1. Determination of the Gibbs Free Energy of Formation of an Oxide	3
2.2. Controlling the Oxygen Partial Pressure to Create or Destroy an Oxide	8
3. Verification of the Oxygen Content of the Cover Gas	14
3.1. Methods of Measuring the Oxygen Content of Gases	14
3.2. Principles of Operation of YSZ Oxygen Sensors	17
4. Control of the Oxygen Content of the Liquid Metal via the Cover Gas	22
4.1. Three Methods of Controlling the Oxygen Content	23
4.1.1. Ultra-High Vacuum	23
4.1.2. Coulometric Titration	23
4.1.3. Gas Dynamic Equilibrium	24
4.2. Considerations of a Gas Dynamic Equilibrium Setup	26
4.2.1. Kinetics of the Dynamic Equilibrium	26
4.2.2. Dilution of Reactive Gases	42
4.2.3. Configuration of a Hydrogen-Water Oxygen Control System	44
4.2.4. Swamping of Leaks and Impurities	48
5. Conclusion	54
6. Recommendations for Future Work	55

Appendix.....	56
References.....	58
Vita.....	Error! Bookmark not defined.

List of Figures

Figure 1: The Richardson-Jeffes diagram.....	9
Figure 2: Times to equilibrium for various H_2/H_2O and CO/CO_2 ratios, as functions of inverse temperature.....	36
Figure 3: Times to equilibrium for the two H_2/H_2O ratios, as functions of temperature.	37
Figure 4: Total equilibrium partial pressure of oxygen as a function of temperature, for a H_2/H_2O ratio of $8 \cdot 10^{-4}$	37

List of Tables

Table 1: Oxygen partial pressure (atmospheres) of oxide formation for several metal oxides of interest.....	12
Table 2: Units of the rate constant, k	28
Table 3: Achievable H_2/H_2O ratios with various methods of adding water vapor to 1% H_2 , balance Ar.....	46
Table 4: Example of an error analysis of the impurities in a system of a gas stream of 1% H_2 , balance Ar, mixed with a gas stream of humidified “pure” Ar	52
Table 5: Kinetic rate constants and equilibrium constants for reactions in the $H_2/O_2/H_2O$ and $CO/O_2/CO_2$ mechanisms	56

List of Symbols

The following table lists some of the symbols used in this document. The units in brackets are meant to be illustrative of the kinds of basic physical quantities involved in the term. The exact units will be stated when the term and symbol is used.

G	=	Gibbs free energy [joules / mole]
H	=	enthalpy [joules/mole]
S	=	entropy [joules/(mole-kelvin)]
T	=	temperature [kelvins, degrees Celsius]
μ	=	chemical potential [joules / (mole or particle)]
R	=	universal gas constant, 8.31451 joules / (mole-kelvin)
$\ln(x)$	=	natural logarithm
$^{\circ}$ (e.g., G°)	=	standard state. The exact meaning depends on context. In general, the following values of variables are taken as standard state values: P = 1 atmosphere T = 293 kelvins
P or p	=	pressure [atmospheres or pascals]
a	=	activity [unitless]
z	=	the number of Faraday equivalents involved in an electrochemical process
F	=	Faraday's constant = 96,500 moles of electrons / coulomb
E	=	voltage or potential [volts]
E^0	=	standard reversible half-cell potential of a substance [volts]

ppmv, ppbv	=	parts per million by volume, parts per billion by volume
c_i	=	concentration of substance i [(M = moles / liter) or (molar fraction, unitless)]
γ_i	=	activity coefficient of substance i [inverse units of concentration]
k	=	rate constant. See Table 2 for units.
K_c	=	equilibrium constant, determined by concentrations [unitless]
K_p	=	equilibrium constant, determined by partial pressures [unitless]
E_a	=	activation energy [joules]
$\exp(x)$	=	exponential function
t	=	time [seconds]

1. Introduction

This thesis addresses the effects and methods of control of the oxygen content of the corrosion environment in molten lead-bismuth eutectic (LBE). LBE is being considered as a possible coolant in future liquid-metal-cooled fast breeder or burner reactors and as a possible coolant and target in future accelerator-driven spallation neutron sources. However, steel surfaces in contact with LBE need to be coated with thin, protective oxide layers in order to prevent the LBE from dissolving the steel. The concentration of oxygen present in the molten LBE determines the kinds of oxides which can form—both beneficial ones and detrimental ones—and various methods exist to determine and control this concentration for maximum net benefit. The concentration of oxygen in the molten LBE is often controlled by controlling the oxygen content in a cover gas. Therefore, this thesis begins with a treatment of the thermodynamics of oxide formation, in the presence of a gas, as a function of temperature and oxygen content. Next, sundry ways to determine and verify the oxygen content are discussed. Then, various methods of controlling the oxygen content are presented and examined, leading to the conclusion that the gas dynamic equilibrium method is probably the best method of oxygen control in most cases. Lastly, key details of the gas dynamic equilibrium method are discussed, such as the kinetics of the chemical reactions in the gas-phase, selection of the best chemical system, dilution and mixing of reactive gases, and the swamping of leaks and impurities.

This thesis focuses on the control of the oxygen content of the cover gas. Therefore, it does not address in detail the thermodynamics and kinetics of the dissolution of the

oxygen from the gas phase into and throughout the liquid LBE. It also does not address the transfer of oxygen from the LBE to the other parts of the system, nor the effect of LBE fluid flow nor temperature differentials between different parts of the system. These topics will be left for future work. The focus here is strictly on the reactions in the gas phase and between the gas phase and solid or liquid surfaces.

2. The Thermodynamics of Oxide Formation

The thermodynamics of oxide formation and disintegration distinguishes the possible from the impossible states. The kinetics determines how quickly the system changes from one state to another. Analysis of both physical considerations is important for the design of LBE systems, both experimental and industrial.

2.1. Determination of the Gibbs Free Energy of Formation of an Oxide

The types of corrosion products which can form are governed by the thermodynamics of the system. For oxygen to react with a metal to form a metal oxide, the sum of the Gibbs free energies of the products (oxide) must be less than the sum of the Gibbs free energies of the reactants (oxygen and metal). In other words, the Gibbs free energy of formation of the oxide at the conditions under consideration (i.e., temperature, concentration, and pressure) must be negative. For a metal, M , undergoing oxidation by oxygen, O , the chemical reaction and Gibbs free energy relations can be expressed as follows:



$$\left[G_{M_AO_B} - \left(A \cdot G_M + \frac{B}{2} G_{O_2} \right) \right] = \Delta G_f \leq 0. \quad \text{Equation 2}$$

Here, the first equation is the chemical balance, with A and B as stoichiometric coefficients, and the second is the Gibbs free energy relation. There are three main ways to determine the Gibbs free energy of formation of a compound, an oxide in this case. The first is to use the second law of thermodynamics, which relates the change in Gibbs free energy to changes in enthalpy and entropy, as follows:

$$\Delta G = \Delta H - T\Delta S. \quad \text{Equation 3}$$

The enthalpies and entropies of formation for many substances have been determined experimentally and are tabulated in many texts, such as *The Oxide Handbook* [1]. The second method requires knowing the oxygen partial pressure of oxide formation. The third method is to make electrochemical measurements. These last two methods are described in greater detail in the following paragraphs.

The second way to determine the Gibbs free energy of formation of an oxide is to relate it to the partial pressure of oxygen in the system. To derive this relation, Equation 3 must be written in terms of chemical potentials, μ . The change in Gibbs free energy is equal to the change in the chemical potential of the system, that is, the chemical potential of the products minus the chemical potential of the reactants. For the reaction of Equation 1, this alternate form is the following:

$$\Delta G = (\mu_{M_A O_B}) - \left(A\mu_M + \frac{B}{2}\mu_{O_2} \right). \quad \text{Equation 4}$$

The chemical potential of a substance changes with temperature and with the activity of the substance, as follows:

$$\mu = \mu^0 + RT \ln(a). \quad \text{Equation 5}$$

Here μ^0 is the chemical potential of the substance at a standard state, R is the universal gas constant, T is the temperature, and a is the activity. Incorporating this relation into the expression for Gibbs free energy change yields the following result:

$$\Delta G = (\mu_{M_A O_B}^0 + RT \ln(a_{M_A O_B})) - \left(A(\mu_M^0 + RT \ln(a_M)) + \frac{B}{2}(\mu_{O_2}^0 + RT \ln(a_{O_2})) \right). \quad \text{Equation 6}$$

Rearranging yields

$$\Delta G = \left[\mu_{M_aO_b}^0 - (\mu_M^0 + \mu_{O_2}^0) \right] + \left[RT \ln(a_{M_aO_b}) - \left(RT \ln(a_M) + \frac{B}{2} RT \ln(a_{O_2}) \right) \right] \quad \text{Equation 7}$$

or

$$\Delta G = \left[\mu_{M_aO_b}^0 - (\mu_M^0 + \mu_{O_2}^0) \right] + RT \ln \left(\frac{a_{M_aO_b}}{a_M^A a_{O_2}^{B/2}} \right). \quad \text{Equation 8}$$

The quantity in the brackets is simply the Gibbs free energy change of the system in the standard state, a tabulated quantity. Also, the activity for a pure solid or liquid is unity; and the activity for an ideal gas is equal to its partial pressure (usually expressed in atmospheres). With these considerations, the change in Gibbs free energy can be expressed as

$$\Delta G = \Delta G^0 + RT \ln \left(\frac{1}{p_{O_2}^{B/2}} \right), \quad \text{Equation 9}$$

or

$$\Delta G = \Delta G^0 - \frac{B}{2} RT \ln(p_{O_2}). \quad \text{Equation 10}$$

At equilibrium, there no longer is any net reaction, so the change in Gibbs free energy, ΔG , is zero. In this case, we can write the above equation as follows:

$$\Delta G^0 = \frac{B}{2} RT \ln(p_{O_2}^0). \quad \text{Equation 11}$$

The partial pressure of oxygen at equilibrium ($p_{O_2}^0$) is the dissociation pressure of the oxide. In other words, it is the partial pressure of oxygen produced by an oxide in equilibrium with its corresponding metal; at this pressure and at this temperature, the oxide does not reduce to the metal nor does the metal oxidize. If this pressure is known,

then Equation 11 represents the second way to determine the Gibbs free energy of formation of an oxide.

A better understanding of Equation 11 can be obtained by substituting it back into Equation 10 to yield the following:

$$\Delta G = \frac{B}{2} RT \ln(p_{O_2}^0) - \frac{B}{2} RT \ln(p_{O_2}), \text{ or} \quad \text{Equation 12}$$

$$\Delta G = \frac{B}{2} RT \ln\left(\frac{p_{O_2}^0}{p_{O_2}}\right) = -\frac{B}{2} RT \ln\left(\frac{p_{O_2}}{p_{O_2}^0}\right)$$

Note that this equation expresses how an increase in partial pressure of oxygen at a given temperature alters the Gibbs free energy change for a metal oxidation reaction. Since any chemical reaction can occur only when the Gibbs free energy change for that reaction is negative, an increase in oxygen partial pressure above the equilibrium partial pressure for the oxide increases the magnitude of this negative quantity, thereby encouraging the reaction (that is, oxidation) to occur. Conversely, if the oxygen partial pressure is below the equilibrium partial pressure, the logarithmic quantity becomes negative and cancels the negative coefficient of the term. In this case, the Gibbs free energy change becomes positive, which means that the reaction goes in reverse: the oxide decomposes back to metal and oxygen.

The third way to determine the Gibbs free energy of formation of an oxide is to make electrochemical measurements. To make such a measurement, an electrochemical cell can be constructed in which the working electrode is fashioned from the metal under consideration. The electrode then reacts electrochemically with oxygen in the electrolyte

to form the metal oxide on the electrode surface. At equilibrium, the oxide is present but does not grow; it is being formed and decomposed at equal rates. The electrical potential of the cell at this equilibrium point is the reversible potential.

For a cell at the equilibrium potential, the first law of thermodynamics can be used to determine the Gibbs free energy of formation. By the first law of thermodynamics, the electrical work being done by the system is equal to the change in energy inside the system. This statement can be written in symbols as follows:

$$\Delta G = -zFE. \quad \text{Equation 13}$$

Here, z is the number of Faraday equivalents used to compose the oxide, F is Faraday's constant, and E is the voltage. Equation 13 is known as the Nernst Law. Now, by Faraday's law of electrolysis, no charge can be flowing through the external circuit at equilibrium. However, if an infinitesimal amount of charge is considered to flow to form an infinitesimal amount of oxide at the equilibrium (reversible) potential, then Equation 13 is valid and can be used to determine the Gibbs free energy of formation of the oxide, as follows:

$$\Delta G_f^0 = -zFE^0. \quad \text{Equation 14}$$

Here, E^0 is the reversible potential, which is often taken to be equivalent to the open-circuit potential. Equation 14 represents the third way to determine the Gibbs free energy of formation of an oxide.

2.2. Controlling the Oxygen Partial Pressure to Create or Destroy an Oxide

Once the Gibbs free energy of formation of an oxide is known via one of the three aforementioned methods, the oxygen partial pressure that is required to form the oxide (at a given temperature) can be easily determined. Essentially, the calculation is running the second method (Equation 11) in reverse: Since the Gibbs free energy of formation is known, the oxygen partial pressure of formation can be calculated. Depending on whether the formation of the oxide is desirable or undesirable, the experimenter can attempt to control the oxygen partial pressure to be respectively greater than or less than this decisive value.

A useful graphical tool for making such comparisons of oxygen pressures is the Richardson-Jeffes diagram [2], which is based on the Ellingham diagram [3]. Figure 1 is the Richardson-Jeffes diagram as reprinted in Darken and Gurry's book [4]. In the Richardson-Jeffes (R-J) diagram, the Gibbs free energies of formation for various metal oxides are plotted against temperature. Note that the relationship between Gibbs free energy of formation and temperature cannot be derived or calculated from the second or third methods—Equation 11 and Equation 14—despite the fact that temperature appears as a variable in Equation 11, since the oxygen partial pressure of formation ($p_{O_2}^0$) is itself a function of temperature. The relationship can be derived from Equation 3 if the changes in enthalpy and entropy are known as functions of temperature, which sometimes is the case. In general, though, the Gibbs free energy of formation for a given oxide is experimentally determined at various temperatures via one or more of the three

methods, and then a line of best fit is drawn through the experimental data points. In their paper, Richardson and Jeffes discuss this line-fitting process and its accuracy [2].

{The author of this thesis does not have permission to publish this figure on the Internet.

Please see Reference [4] for the original publication of the figure.}

Figure 1: The Richardson-Jeffes diagram, as published in Reference [4], and reprinted with permission. This diagram plots the standard free energy of formation of many metal oxides as a function of temperature.

The oxidation reactions plotted in the R-J diagram are written to be balanced for one mole of oxygen gas, such that the quantity $B/2$ equals unity. In this case, the Gibbs free energy of formation, ΔG^0 , equals the quantity $(RT \ln p_{O_2}^0)$, according to Equation 11.

The diagrams are used as follows: To know whether or not a given metal will oxidize at a certain temperature and in an environment with a certain partial pressure of oxygen (p_{O_2}), it suffices to determine whether the quantity $(RT \ln p_{O_2})$ for this given situation is above or below the corresponding oxide line on the diagram. Essentially, this process is a quick, graphical way of determining if ΔG in Equation 10 and Equation 12 is negative or positive. If the quantity $(RT \ln p_{O_2})$ is above the line, then the quantity $(\Delta G^0 - RT \ln p_{O_2})$ is negative, so ΔG is negative, so the metal will oxidize. Conversely, if it is below, then the quantity $(\Delta G^0 - RT \ln p_{O_2})$ is positive, so ΔG is positive, so the metal will not oxidize and any oxide that happens to be present will decompose. In this latter case, one can consider that the gaseous environment does not contain enough oxygen to oxidize the metal at the given temperature. Lastly, if two or more metals are in the oxidizing environment, the R-J diagram indicates which elements will likely oxidize first, being those for which the Gibbs free energy change is more negative.

The R-J diagram, especially as reprinted by Darken and Gurry [4], incorporates a useful graphical feature for determining the oxygen partial pressure at any given point on the diagram. The ordinate of the R-J diagram is $(RT \ln p_{O_2})$, which is a function of temperature, the abscissa. Therefore, Richardson and Jeffes created a transparent overlay for the diagram, consisting of logarithmically spaced, parallel diagonal lines of constant

oxygen partial pressure. Darken and Gurry incorporated this overlay as a nomogram; that is, they reprinted this overlay as sidebars, to be connected with a straightedge. In this way, the oxygen partial pressure of any point on the R-J diagram can be read off using the overlay or sidebar, without calculation. The R-J overlay also contains gridlines for constant CO/CO₂ ratio; the Darken and Gurry reprint includes this ratio and also a H₂/H₂O ratio. The meaning and utility of these ratios and gridlines will be explained in the later section on the gas dynamic equilibrium method of oxygen control.

From the R-J diagram, it is clear that the oxygen partial pressures of formation of the metal oxides of interest in a LBE system are very low in comparison with the oxygen content of air, which is about 21%, or $2.1 \cdot 10^{-1}$ atmospheres partial pressure (or mole fraction). Table 1 lists the oxygen partial pressures of formation for several of these oxides. Note that, according to the table, lead oxide (PbO) is more stable than bismuth oxide (Bi₂O₃). Therefore, when molten LBE is exposed to excessive oxygen (such as in air), the lead will have to oxidize almost completely before the bismuth begins to oxidize. Therefore, the level of oxygen required to oxidize the lead is the maximum amount of oxygen that is tolerable in a practical LBE system.

These partial pressures are unattainable by even the best gas purification available today. For reference, the guaranteed maximum oxygen content of research purity (99.9999% purity) argon, supplied by Matheson Tri-Gas, was 0.5 ppm as of February 2006 [5]. This figure translates into a maximum possible oxygen partial pressure of $5 \cdot 10^{-7}$ (atmospheres), which is at least seven orders of magnitude higher than the greatest

oxygen partial pressure of formation listed in Table 1. This fact means that gas purification is not viable as a method to lower the oxygen partial pressure below the partial pressure of oxide formation for any of the oxides of interest. Thus, with this method there is no possibility of selectively oxidizing some metals and not others; all the metal oxides will form under conditions of such relatively high oxygen partial pressure. To be able to reach the low oxygen partial pressures required for selective oxidation, alternate methods of controlling oxygen partial pressure must be used. These alternate methods will be discussed in detail in a later section.

Table 1: Oxygen partial pressure (atmospheres) of oxide formation for several metal oxides of interest. Data taken from indicated references.

Oxide	Temperature	
	400°C	600°C
Bi ₂ O ₃ [6]	$5.0 \cdot 10^{-21}$	$4.0 \cdot 10^{-14}$
Fe ₂ O ₃ (from Fe ₃ O ₄) [4]	$1.7 \cdot 10^{-22}$	$9.6 \cdot 10^{-15}$
PbO [2]	$9.3 \cdot 10^{-25}$	$9.5 \cdot 10^{-17}$
NiO [2]	$2.5 \cdot 10^{-28}$	$1.7 \cdot 10^{-19}$
FeO [2]	$1.7 \cdot 10^{-34}$	$2.9 \cdot 10^{-25}$
Fe ₃ O ₄ (from FeO) [2]	$4.0 \cdot 10^{-36}$	$5.2 \cdot 10^{-25}$
Cr ₂ O ₃ [2]	$9.2 \cdot 10^{-50}$	$1.6 \cdot 10^{-36}$
MnO [2]	$2.5 \cdot 10^{-53}$	$2.8 \cdot 10^{-39}$
SiO ₂ [2]	$1.6 \cdot 10^{-58}$	$2.8 \cdot 10^{-43}$

It should be pointed out that the above discussion of oxide thermodynamics assumes that the metal and gas are in direct contact with each other. For example, a test coupon of

nickel might be put into a furnace and heated in the presence of an oxygen-containing gas. The thermodynamics, then, describes the reaction between the surface of this nickel sample and the oxygen gas. In the case of an LBE system, however, the steel surfaces are, in general, not in contact with the gas but rather with the liquid LBE. The oxidation reactions, therefore, occur with the oxygen dissolved in the LBE. This thesis will not address this issue, since the focus is on control of the oxygen content of the cover gas, but it is an important distinction to keep in mind.

3. Verification of the Oxygen Content of the Cover Gas

Since the types of oxides formed in a LBE system depend on the oxygen concentration or partial pressure of the system, it would be helpful to be able to verify what the oxygen content is as a function of time and/or location in the system. For relatively high oxygen concentrations of 100 ppb or greater, several accurate measurement techniques exist. For the low oxygen concentrations in the range of interest for control of oxide formation— 10^{-21} to 10^{-30} mole fraction—the measurement options are far fewer. The range of techniques for oxygen content measurement is explored in the following sections.

3.1. Methods of Measuring the Oxygen Content of Gases

In laboratory experiments of oxygen solubility in liquid metals [7], scientists have the luxury of being able to quench their samples of liquid metal—thereby locking in the oxygen—and analyze them in a gas chromatograph or mass spectrometer for their oxygen content. For a practical LBE system, however, online oxygen measurement is needed. Three methods for online oxygen measurement will be discussed here. The first is the membrane method. One company which uses this technology is Orbisphere [8]. In this method, the sensor is electrochemical: a working electrode and a counter electrode are separated by an electrolytic solution. A gas-permeable membrane separates the solution from the environment in which the oxygen measurement is to be taken. Oxygen diffuses through the membrane and into the electrolyte, where it is reduced, presumably at the working electrode, since it is made of a noble metal. The electrical current which passes through the electrochemical cell is proportional to the oxygen in the electrolyte, which is proportional to the oxygen in the environment. The membrane method can be used for

measuring oxygen in gases or in solutions. However, the maximum operating temperature of the sensor is only about 60°C, well below the operating temperature of a LBE system (~500°C). This maximum temperature is probably defined by the membrane; at higher temperatures, the membrane probably first degrades and then decomposes. The electrolyte might also boil at high temperatures. Also, the lowest oxygen content which can be measured with this method is 0.25 Pa in gas or 0.1 ppb in solution, neither of which is close to the oxygen range of interest for LBE systems. Therefore, the electrochemical membrane method is largely unsuitable for use in a LBE system.

A second method for measuring oxygen content is optical and uses fluorescence. A company which uses this method is Ocean Optics [9]. The following description of the measurement process of their FOXY oxygen sensors is taken from their website:

FOXY Fiber Optic Oxygen Sensors use the fluorescence of a ruthenium complex in a sol-gel to measure the partial pressure of oxygen:

1. The pulsed blue LED [light-emitting diode] sends light, at ~475 nm, to an optical fiber.
2. The optical fiber carries the light to the FOXY probe. The distal end of the probe tip consists of a thin layer of a hydrophobic sol-gel material. A ruthenium complex is trapped in the sol-gel matrix, effectively immobilized and protected from water.
3. The light from the LED excites the ruthenium complex at the probe tip.
4. The excited ruthenium complex fluoresces, emitting energy at ~600 nm.

5. If the excited ruthenium complex encounters an oxygen molecule, the excess energy is transferred to the oxygen molecule in a non-radiative transfer, decreasing or quenching the fluorescence signal. ... The degree of quenching correlates to the level of oxygen concentration or to oxygen partial pressure in the film, which is in dynamic equilibrium with oxygen in the sample.
6. The energy is collected by the probe and carried through the optical fiber to the spectrometer. The A/D converter converts this analog data to digital data your PC can understand. This data is then displayed in [special software].

The oxygen diffuses from the environment, through the sol-gel, and onto the probe tip, so this sensor can work in both liquids and gases. However, the maximum operating temperature of these probes is only 80°C, and the lowest detectable limit is only 0.03 ppm. Therefore, this type of oxygen sensor is also unsuitable for use in a LBE system.

A third method for measuring oxygen content is the solid-electrolyte oxygen sensor. Several companies manufacture this type of sensor; one of them is Cambridge Sensotec Ltd [10]. The most commonly used type of solid electrolyte is stabilized zirconia (ZrO_2), although doped thoria (ThO_2) has better operation at higher temperatures [11, 12]. To stabilize the cubic phase of zirconia and prevent it from transitioning to the monoclinic phase (the stable phase below 1170°C) [13], the stabilizing oxide could be calcia (CaO), magnesia (MgO), or yttria (Y_2O_3) [7]. Yttria-stabilized zirconia (YSZ) seems to be the predominantly used electrolyte today. The operating temperature range of these sensors is relatively high—at least from 340°C to over 900°C [14]—although the kinetics of the sensor may be poor at the lower temperatures. The sensors can be designed to measure oxygen in either liquid or gas. Commercially available, air-referenced sensors are

accurate only down into the range of parts per billion, but they still can provide a rough relative measurement of oxygen into the range of 10^{-26} mole fraction [10]. Non-commercial, laboratory-built sensors with metal/metal-oxide sensors have apparently been used with accuracy well into the range of interest for a LBE system [6, 14-20]. The conclusion is that the solid-electrolyte oxygen sensors are the best, if not the only, sensors available for oxygen measurements in LBE systems. The yttria-stabilized zirconia (YSZ) oxygen sensor will be described in more detail in the next section.

3.2. Principles of Operation of YSZ Oxygen Sensors

A YSZ oxygen sensor works as follows. At high temperatures, the solid electrolyte becomes ionically conductive but not appreciably electronically conductive. (See Patterson's paper [12] for a plot of the electrolytic domain of calcia-stabilized zirconia; the plot for yttria-stabilized zirconia should be similar.) On one side of the solid electrolyte, a reference environment—with known oxygen content—is used. On the other side is the unknown environment—with unknown oxygen content. In most cases, the reference environment is chosen to have a greater oxygen content than the unknown environment. In such cases, then, the oxygen diffuses through the solid electrolyte in the direction of the concentration gradient, that is, from high concentration on the reference side to low concentration on the unknown side. However, the solid electrolyte is only ionically conductive; it does not pass uncharged atoms. Therefore, the oxygen on the reference side is reduced to O^- ions, passes through the solid electrolyte, and finally oxidizes back to neutrality. For this ionic conduction to work, however, three other important components must be present: (1) a catalytic and conductive electrode on the reference side to reduce the oxygen atoms and remove the electrons, (2) an external

circuit to conduct the electrons to the unknown side, and (3) a catalytic and conductive electrode on the unknown side to provide electrons and oxidize the oxygen ions. If a high-impedance electrometer is put into the external circuit, practically no current flows; instead the open-circuit voltage of the electrochemical system under this concentration is measured. The open-circuit voltage is related to the concentration difference between the reference and unknown sides of the solid electrolyte. Both the reference side and the unknown side of the sensor can be either gas or liquid.

The ideal relationship between the open-circuit voltage and the concentration difference can be derived as follows. The chemical reaction here is the dissociation and ionization of oxygen so that it can pass through the YSZ: $\frac{1}{2}\text{O}_2 \Leftrightarrow \text{O}^{-2} + 2\text{e}^{-}$. Comparing this reaction with Equation 1, we see that A equals zero and B equals unity. We can then plug Equation 13 into Equation 12 and rearrange it to give the Nernst equation, which relates the logarithm of the ratio of the oxygen partial pressures to the open-circuit voltage:

$$-zFE = \frac{B}{2}RT \ln\left(\frac{p_{\text{O}_2}}{p_{\text{O}_2}^{\text{ref}}}\right) = -\frac{B}{2}RT \ln\left(\frac{p_{\text{O}_2}^{\text{ref}}}{p_{\text{O}_2}}\right), \text{ or}$$

$$E = \frac{RT}{zF} \ln\left(\frac{p_{\text{O}_2}^{\text{ref}}}{p_{\text{O}_2}}\right)^{\frac{1}{2}}. \quad \text{Equation 15}$$

Here, $p_{\text{O}_2}^{\text{ref}}$ stands for the oxygen partial pressure on the reference side. Actually, though, the more general form of Equation 15, which uses oxygen activities instead of partial pressures, is more appropriate in the case of measurements made in liquid metal. Essentially, this form is derived from Equation 8 without making the substitution of partial pressures for activities:

$$E = \frac{RT}{zF} \ln \left(\frac{a_{O_2}}{a_{O_2}^{ref}} \right)^{1/2} . \quad \text{Equation 16}$$

Here, the activity of a gas reference can again be assumed to be the partial pressure of the oxygen in the gas (assuming ideal gas behavior). The activity in a liquid metal or metal/metal-oxide mixture should be calculated by multiplying the oxygen concentration in the metal or mixture by the appropriate value of the activity coefficient:

$$a_{O_2} = \gamma_{O_2} c_{O_2} , \text{ or} \quad \text{Equation 17}$$

$$a_O = \gamma_O c_O .$$

Note that the oxygen concentration in a liquid metal is in the form of monatomic oxygen rather than diatomic oxygen. The relationship between the activities is derived from the reaction $\frac{1}{2}O_2 \Leftrightarrow O$, which yields the following relationship of the activities: $a_O = (a_{O_2})^{1/2}$. For an example, if the reference is air at atmospheric pressure and if the unknown environment is liquid LBE, Equation 16 would be modified to yield the following:

$$E = \frac{RT}{zF} \ln \left(\frac{\gamma_{O \text{ in LBE}} c_O}{(0.21)^{1/2}} \right) . \quad \text{Equation 18}$$

For making measurements of relatively high oxygen concentrations (that is, in the parts-per-trillion range and above), air or pure oxygen is often used as a reference gas. For making measurements of lower oxygen concentrations, such as in a LBE system, it is advantageous to use a known metal/metal-oxide mixture as the reference. Some metal/metal-oxide references used in the past have been Sn/SnO₂, Bi/Bi₂O₃ and In/In₂O₃

[6, 16, 18, 19, 21]. By the R-J diagram, the oxygen partial pressure of such a mixture at equilibrium is known. Since the oxygen concentration in such a mixture is closer in magnitude to the unknown concentration than is the concentration of a gas reference, the open-circuit voltages that will be measured will show greater variation with concentration difference—that is, the sensor will have greater sensitivity. This fact should be evident from considering Equation 16. The derivative of the logarithmic function is $1/x$, so the change in voltage, corresponding to a change in oxygen activity in the LBE, is the greatest when the argument of the logarithmic function is close to unity

A complication with the metal/metal-oxide reference is that, typically, the metal/metal-oxide reference is not isolated but is open to air via a channel [6]. In this case, three assumptions are being made about the operation of the reference. First, it is assumed that the metal oxide floats on the surface of the liquid metal. Actually, this feature is usually true for metals and their oxides; if it is not, another metal/metal-oxide system should be chosen. Second, it is assumed that the concentration of oxygen within the liquid metal is about equal to the partial pressure of formation of the oxide—not the partial pressure in the air (~ 0.21 atm) in contact with the surface of the metal. In essence, the metal oxide on the surface of the liquid metal screens it from direct contact with the air. The oxygen in the air is forced to diffuse through the oxide layer in order to contact the liquid metal and oxidize it. The third assumption is based on the second: it is also assumed that the liquid metal has not yet completely oxidized. In other words, when the metal/metal-oxide reference is in contact with air, it is a dynamic system. It is always oxidizing. This fact means that, periodically, it will be necessary to replace the metal/metal-oxide

reference, if other engineering factors do not first precipitate an earlier replacement of the entire sensor.

4. Control of the Oxygen Content of the Liquid Metal via the Cover Gas

Achieving oxygen saturation in a liquid metal is easy: simply expose it to air. The oxide is usually less dense than the metal so it will float on the surface of the liquid metal and screen it from direct contact with the air. Even if there are kinetic limitations of oxygen diffusion through the oxide, it can be assumed that the oxygen concentration in the liquid metal underneath the oxide is almost equal to the partial pressure of formation of the oxide at the experiment's temperature. If this metal can be collected, it can be sampled and analyzed for its oxygen content. Chang, Fitzner, and Zhang mention six experimental methods of determining the solubility of oxygen in various liquid metals [7], and all but one of these methods (coulometric titration) involve sampling the liquid metal, cooling it, and analyzing it in a gas chromatograph or mass spectrometer. The truly difficult problem, however, is to control the oxygen content of a liquid metal well below its oxidation limit. In practical LBE systems, this problem is usually compounded by the large volume of liquid metal and by dynamic effects, such as forced or convective liquid metal flow, dissolution and precipitation reactions, and consumption of oxygen by the formation of oxides on steel surfaces. This oxygen-control problem is very difficult, but solving it begins with controlling the oxygen content of the cover gas. Therefore, controlling the oxygen content of the cover gas is the subject of the following sections.

4.1. Three Methods of Controlling the Oxygen Content

Three methods which might be able to control the oxygen content in a liquid LBE system are ultra-high vacuum, coulometric titration, and gas dynamic equilibrium. The merits and difficulties of each method are discussed below.

4.1.1. Ultra-High Vacuum

Controlling the oxygen partial pressure with an ultra-high vacuum system seems as though it would be the most straightforward method: just use a pressure gage to measure the approximate oxygen partial pressure. It would avoid the complications of dealing with chemical reactions (as in the gas dynamic equilibrium method, described below) or of interpreting sensitive coulometric titration data. Unfortunately, an ultra-high vacuum system typically is able to reach only to about 10^{-7} torr ($1.31 \cdot 10^{-10}$ atm) regularly and with ease. However, this pressure is not low enough to ensure that the oxygen levels are below the oxidation line for PbO, at about $1 \cdot 10^{-16}$ atm around 600°C. (See Table 1.) Therefore, this method cannot be used to control the oxygen partial pressure in an LBE system.

4.1.2. Coulometric Titration

Coulometric titration is the addition or removal of oxygen to the LBE from an oxygen source via a solid-oxide electrolyte such as YSZ. Chang, et al., describe the concept in their paper [7]. The principle is similar to that of YSZ oxygen sensors: oxygen passes through the YSZ electrolyte under the influence of both a concentration gradient and an applied voltage. In the oxygen sensor, no current is allowed to flow, and the open circuit voltage is measured. In the titration electrochemical cell, a voltage is applied to the

electrolyte and current is forced to flow, causing oxygen to be either added or removed from the LBE, depending on the voltage applied and the relative concentration difference. By measuring the current, Faraday's law of electrolysis can be used to calculate the amount of oxygen that was transferred through the YSZ electrolyte. The difficulty with this method is that it might not be able to transfer oxygen in and out of the LBE system quickly enough when large quantities are used, as in a practical system. For example, Ghetta, et al., used this method with only 0.5 liters of LBE [22]. Johnson, et al., indicated that an electrochemical method was used during tests at IPPE, in Russia, but gives no details [23].

4.1.3. Gas Dynamic Equilibrium

A popular way to control the oxygen content of an environment is to use the gas dynamic equilibrium method. In this method, several reactive gases are mixed in predetermined proportions. When the gases fully react with one another—that is, when they are in dynamic equilibrium—they produce a specific partial pressure of oxygen in the product gas mixture. The exact amount of oxygen in the product mixture is determined by the ratio of the reactant gases. This product mixture is brought into contact with the LBE by bubbling the gas through the LBE or simply by using the mixture as a cover gas on an enclosed free surface of the LBE. It is assumed that the oxygen content of the LBE then equilibrates to the oxygen content of the cover gas, in a timely fashion. By the continuous blowing or bubbling of the gas, the oxygen content of the gas remains fixed and is not altered by the removal or addition of oxygen from or to the LBE.

Two popular systems of gases are the hydrogen—oxygen—water system ($\text{H}_2/\text{O}_2/\text{H}_2\text{O}$) and the carbon-monoxide—oxygen—carbon-dioxide system ($\text{CO}/\text{O}_2/\text{CO}_2$). The chemical reactions for these systems are respectively as follows:



The Gibbs free energy changes and corresponding equilibrium constants as functions of temperature for these reactions are published in the JANAF tables and republished in Glassman's book on combustion [24, 25]. They can also be determined from the R-J plot [2, 4] by using the overlay or sidebars, which contain logarithmically spaced lines of constant $\text{H}_2/\text{H}_2\text{O}$ (Darken & Gurry's reprint, only) and CO/CO_2 (both) ratios as functions of temperature. Note that the JANAF values are for one mole of product gas (H_2O or CO_2), whereas the R-J diagram values are for one mole of oxygen gas. Although the two sources do not exactly agree, they are at worst within an order of magnitude of each other, which is close because of the logarithmic dependence of Gibbs free energy on oxygen.

Since the target oxygen partial pressures in an LBE system are so low (see the previous discussion), it can be helpful to consider the reactions in reference to their limiting cases. For example, if pure hydrogen was blown over the free surface of the LBE, all of the oxygen in the LBE would eventually react with the hydrogen to form water vapor, which would be blown out of the system. (Note that the purity of the hydrogen is with reference to the presence of other reactive gases and not a non-reactive diluent such as argon.) On the other hand, if pure water vapor was blown over the LBE, the water molecules would

dissociate to yield a particular partial pressure of oxygen, determined by the temperature of the gas. Although very low compared to the oxygen content of air, this oxygen partial pressure would certainly be well above the minimums for oxidation of the metals in a LBE system, as can be seen from the R-J diagram. This oxygen would, therefore, react with the LBE to form lead and bismuth oxides. The hydrogen atoms remaining from the dissociation of the water molecules would be blown out of the system, most likely in the form of radicals such as the hydroxide radical (OH) or perhaps as hydrogen peroxide. When the hydrogen and water vapor are mixed together, the oxygen consumption and production reactions balance each other, and the resulting oxygen partial pressure is somewhere between the two extremes. Note that, if hydrogen was mixed with air or with pure oxygen, the hydrogen would react with the oxygen to form water until the resulting gas mixture was a mixture of hydrogen and water vapor, at which point the above discussion would become valid.

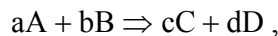
4.2. Considerations of a Gas Dynamic Equilibrium Setup

4.2.1. Kinetics of the Dynamic Equilibrium

The R-J diagram's overlay or sidebars and the JANAF tables indicate the thermodynamic balance between H₂ and H₂O and between CO and CO₂. However, the thermodynamics alone give no indication of the kinetics of these dynamic equilibria. The kinetics of these dynamic equilibria have been largely overlooked in the recent literature of nuclear materials testing, with, perhaps, a negative impact on the reliability and repeatability of the results [6, 15-39]. The following paragraphs address the kinetics concerns of the gas dynamic equilibrium method and proffer one possible solution.

The essential kinetic concern is that, although the thermodynamics might indicate that a particular ratio of reactive gases (either H_2 and H_2O or CO and CO_2) should yield a particular partial pressure of oxygen at a particular temperature, the gases might not react with each other quickly enough to attain this predicted value of oxygen partial pressure in a reasonable timeframe. According to Glassman [25], a stoichiometric mixture of hydrogen and oxygen will not react, at any pressure, below a temperature of 675 K (about $400^\circ C$), assuming no catalyst, such as platinum, is present. The implication is that, below $400^\circ C$ at least, the gas dynamic equilibrium method is completely useless for controlling oxygen partial pressure. In practice, the H_2/H_2O system cannot be equilibrated in less than one minute below approximately $900^\circ C$; and the CO/CO_2 system (using research-grade purity gases with less than 20 ppmv total of hydrogen and water impurity [5, 25]) cannot equilibrate at low CO/CO_2 ratios in less than four minutes below approximately $1300^\circ C$, which is above the maximum operating temperature of many tube furnaces. The theory and evidence for these statements will be discussed below.

First, a brief review of chemical reaction kinetics will lay the foundation for the subsequent discussions. According to the law of mass action, which has been confirmed experimentally, the rate of a chemical reaction (defined as the rate of consumption of one of the reactants) is proportional to the product of the concentrations of the reactants. Reactants with coefficients other than unity take their coefficients as exponents in this proportionality (i.e., multiplication is a succession of additions) [25, 40]. In symbols, for a given reaction such as



where the upper case letters are the chemical species and the lower case letters are the stoichiometric coefficients, the forward rate equation is as follows:

$$\frac{d}{dt}([A]) = \frac{d}{dt}([B]) = -k[A]^a[B]^b . \quad \text{Equation 21}$$

Here, the brackets denote the concentration of the chemical species inside the brackets (e.g., $[A]$ is the concentration of species A). The constant of proportionality, k , is called the rate constant. Usually, the concentrations in Equation 21 are functions not only of time but also of initial concentration, depending on the order of the reaction. In all cases, though, the rate constant, k , is a constant.

The units of the rate constant, k , depend on the order of the reaction. They can be summarized as follows [40]:

Table 2: Units of the rate constant, k

<u>Order</u>	<u>Units of k</u>
0	mole liter ⁻¹ sec ⁻¹
1	sec ⁻¹
2	liter mole ⁻¹ sec ⁻¹
3	liter ² mole ⁻² sec ⁻¹

Sometimes the rate constant is written as k_f , to denote it as the forward rate constant and thereby to distinguish it from the backward rate constant, k_b , which is the rate constant for the reverse chemical reaction. The two constants are related to each other, because at

equilibrium, the forward and reverse reaction rates must be equal. Algebraic derivation yields the relation

$$\frac{k_f}{k_b} = K_c \left\{ = \frac{[C]^c [D]^d}{[A]^a [B]^b} \text{ for this reaction, for example} \right\}, \quad \text{Equation 22}$$

where K_c is the equilibrium constant based on concentrations. K_c is related via the ideal gas law to K_p , the equilibrium constant based on pressures, which is in turn related to the change in Gibbs free energy for the reaction [25, 40]—a thermodynamic quantity:

$$K_p = K_c (RT)^{(c+d)-(a+b)} = \exp\left(-\frac{\Delta G^0}{RT}\right). \quad \text{Equation 23}$$

Note that, although the thermodynamic equilibrium constant appears here in relation to kinetics, it states only the ratio of the rate constants and cannot indicate anything of their individual magnitudes, which are the quantities of interest for kinetics.

Though the rate constant is not a function of time, it is a function of temperature. In the 1880s, Svante Arrhenius showed how the assumption of an activation energy barrier, E_a , for chemical reactions between molecules resulted in an exponential dependence of the rate constant on temperature:

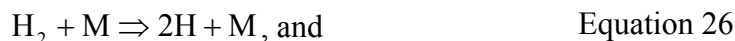
$$k = k(T) = A \exp\left(-\frac{E_a}{RT}\right). \quad \text{Equation 24}$$

Here, A is called the kinetic pre-exponential factor. Experimentally, it has been shown that A depends on temperature, too, especially for recombination reactions—when radicals recombine to form stable molecules—and for radical reactions with low activation energies [25]. In these cases, it is helpful to remove this temperature dependence explicitly, leaving A to be just a constant:

$$k = k(T) = A \cdot T^n \cdot \exp\left(-\frac{E_a}{RT}\right). \quad \text{Equation 25}$$

Here, n is an experimentally determined exponential factor of the temperature. Frequently, n is one half. Equation 25 is called the modified Arrhenius rate-constant equation.

When hydrogen, oxygen, and water react with each other, the molecules must first dissociate into radicals before they can combine into other products. The forward reaction—that is, the reaction of hydrogen and oxygen—consumes the oxygen that is in excess of the equilibrium concentration. The key initiating step for this forward reaction is the production of hydrogen radicals, H, by one of the following two reactions:



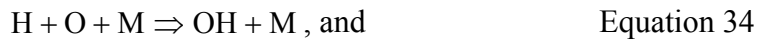
At lower temperatures, Equation 27 is the more likely reaction. The key chain reaction step then follows from this radical:



Note that two radicals—O and OH—are formed from the one H radical; this reaction is, therefore, called a chain branching reaction. The following three reactions perpetuate the chain reaction:



There are two types of reactions which can end the chain reaction: reactions between radicals in the gas phase and reactions between radicals in contact with the container wall. Above 875 K and in atmospheric-pressure flames, the reaction is terminated in the gas phase by the recombination of the radicals back into stable molecules. This recombination requires the presence of a third, non-reactive molecule (M) to absorb the exothermic heat of reaction when the radicals combine. Without this third molecule, the product molecule is likely to dissociate again quickly because of the excess heat. These gas-phase reactions are as follows:



Note that these are tri-molecular reactions, which have a lower probability of occurrence than the bi-molecular chain reactions. Therefore, their reaction rate constants are expected to be small, such that these termination reactions do not dominate until the chain reactions have slowed due to the consumption of reactants. Other termination reactions involve the container wall: either the O, H, and OH radicals directly contact the wall and form stable products, or the relatively stable hydroperoxy radical (HO_2) is formed in the gas phase and diffuses to the wall to dissociate and reconfigure into stable products. Again, the diffusion process is relatively slow, so these termination reactions do not dominate until after the chain reactions have slowed. Note that the major result of all of these reactions is the production of water, according to the reactions of Equation 30 and Equation 35.

The reverse reaction is the dissociation of water back into oxygen and hydrogen, thus providing oxygen when its level is below that of the equilibrium concentration. The primary dissociation reactions are probably Equation 31 and the reverse of Equation 30. In these reactions, the water molecules are split up when hit by either oxygen or hydrogen radicals, which can be formed—albeit at slow rates—by several other possible reactions.

Some of the most important reactions that can occur in the $H_2/O_2/H_2O$ system are listed in Table 5 in the Appendix. Together, the set of reactions is called the mechanism for the H_2-O_2 system. With each reaction is listed its corresponding forward and backward reaction rate constants, as well as its thermodynamic equilibrium constant, for a temperature of 1373 K (1100°C), which is a common maximum continuous operating temperature for tube furnaces. Most of the rate constants follow an Arrhenius or modified Arrhenius temperature dependence. Table 5 in the Appendix also includes the mechanism for the $CO-CO_2$ system. The table was derived from Table 1 in Appendix B of Glassman's book and from the 1998 edition of the NIST-JANAF thermodynamic tables [25, 41].

The set of reactions in a mechanism, along with their rate constants, enable the calculation of the concentrations of the various species in a given system as a function of time. Essentially, the calculation begins by specifying what the initial concentrations of reactants should be. In the case of the H_2/H_2O gas dynamic equilibrium, the initial concentrations of H_2 and H_2O would be specified to reflect the ratio of these two gases;

the concentrations of all other species would be zero. Then, the rate equations for all of the reactions in the mechanism are solved simultaneously to determine the concentrations of all of the possible species are calculated. However, since the concentrations change with time, the rate equations need to be solved for very small time steps. By solving the system of rate equations repeatedly over a series of many time steps, the concentrations of all of the species as functions of time can be determined. When the values of the concentrations of the species no longer change, then the system can be said to have reached equilibrium.

Though theoretically these calculations can be done by hand, it is much more practical to do them on a computer. One program which can do these calculations is the *Zero: A Zero-Dimensional Kinetics Simulator* program, written by David G. Goodwin at the California Institute of Technology in October, 2001 [42]. It is a perfectly stirred reactor program based on the freeware computer program *Cantera* (www.cantera.org). This program is called a zero-dimensional program because it calculates the concentrations solely as functions of time and not of spatial position. This program does not use its own mechanism but calls a separate mechanism file, to be supplied by the user. The mechanism used by the author was the GRI-Mech 3.0 file, which was created on March 12, 1999, by researchers from the Gas Research Institute (now the Gas Technology Institute), the University of California at Berkeley, Stanford University, SRI International, and the University of Texas at Austin [43].

To evaluate the performance of the H₂/H₂O and CO/CO₂ gas dynamic equilibrium methods of oxygen control, two cases of each system were run through the *Zero* program over a range of temperatures. The first case was for equal quantities of H₂ and H₂O or of CO and CO₂. The second case was for H₂/H₂O and CO/CO₂ ratios which yielded an oxygen partial pressure of about 5·10⁻²² atmospheres. At 500°C, this oxygen level is a point that falls between the oxidation lines for PbO and NiO and thus might be a target point for oxygen control in a practical LBE system. For this second case, the H₂/H₂O ratio was found to equal approximately 8·10⁻⁴, and the CO/CO₂ ratio was found to equal approximately 2·10⁻⁴, as determined from the R-J diagram reprint in Darken and Gurry's text. The oxygen partial pressure corresponding to these H₂/H₂O and CO/CO₂ ratios was calculated using the NIST-JANAF tables as being about 4·10⁻²¹ atmospheres—which is about one order of magnitude lower than the value of 5·10⁻²² atmospheres as determined by the R-J diagram. This difference could be due to the inaccuracy of reading off the H₂/H₂O and CO/CO₂ ratios on the R-J diagram or to the differences in accuracy between the data in the R-J diagram and the newer data in the NIST-JANAF tables. In any case, although an order of magnitude seems like a large difference, in practical fact, it is not: both the R-J-derived point and the NIST-JANAF-derived point lie very close to each other on the R-J diagram, due to the logarithmic dependence of the Gibbs free energy on oxygen partial pressure. (See Equation 11.) Both points are certainly well below the PbO oxidation line and well above the NiO oxidation line.

For each of the cases that were run through the *Zero* program, the equilibrium concentration of oxygen at each temperature point was determined, if possible. The

program was run to yield data only for the first 1000 seconds of the reactions, so some of the cases were unable to equilibrate within this timeframe at the lower temperatures. For the sake of this evaluation, the system was considered to be at equilibrium when the first significant digit no longer changed with time. In practical LBE systems, this level of accuracy would be more than sufficient for oxygen control, due to the logarithmic dependence of the Gibbs free energy on oxygen partial pressure.

Figures 2 through 4 show the results of the *Zero* modeling. Note that only data for those cases which equilibrated within the 1000 seconds of the simulation are plotted. Figure 2 is a plot of the equilibrating time as a function of inverse temperature. The reason for this format is that a straight line is expected on this plot, for a reaction with an Arrhenius rate constant. According to Latham [40], the half-life of a reaction—that is, the time to 50% completion of the reaction—is inversely proportional to the rate constant. This relation is true regardless of the order of the reaction, as long as one is comparing results for reactions with the same initial concentrations of reactants and products. For the *Zero* modeling of each case of the systems, the same initial concentrations were used throughout the temperature range. The half-life in Latham's proportionalities can be replaced by the time to 99% completion of the reaction (or any other such representation of equilibrium) completion without changing the proportionality; it is the time to equilibrium, not the half-life, which is of interest here. Next, the Arrhenius relation can be substituted for the rate constant in the proportionality. Further manipulation yields an expression showing the relation between the logarithm of time as a function of inverse

temperature. With C representing the constant of proportionality, the algebra is as follows:

$$t_{\text{equilibrium}} = C \cdot \left(\frac{1}{k} \right) = C \cdot \left(\frac{1}{A e^{-(E_a/RT)}} \right) = \frac{C}{A} \cdot e^{(E_a/RT)}$$

Equation 36

$$\log_{10}(t_{\text{equilibrium}}) = \left(\frac{E_a \cdot \log_{10}(e)}{R} \right) \cdot \frac{1}{T} + \log_{10}\left(\frac{C}{A}\right).$$

Figure 2 shows that all of the four cases mostly follow this linear relationship. (Note that the dashed lines are not linear fits but are simply aids for viewing the plot.)

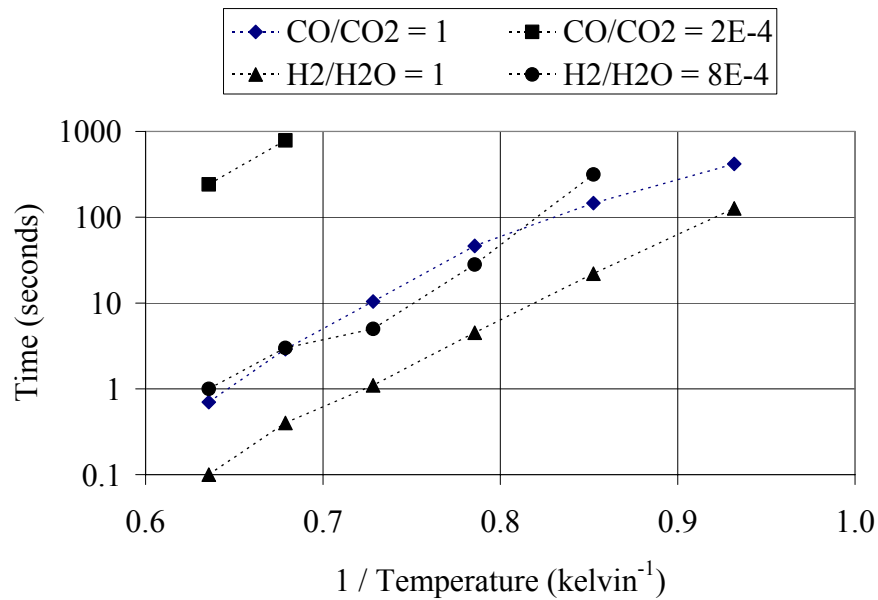


Figure 2: Times to equilibrium for various H₂/H₂O and CO/CO₂ ratios, as functions of inverse temperature. The times were calculated by the *Zero* program [42].

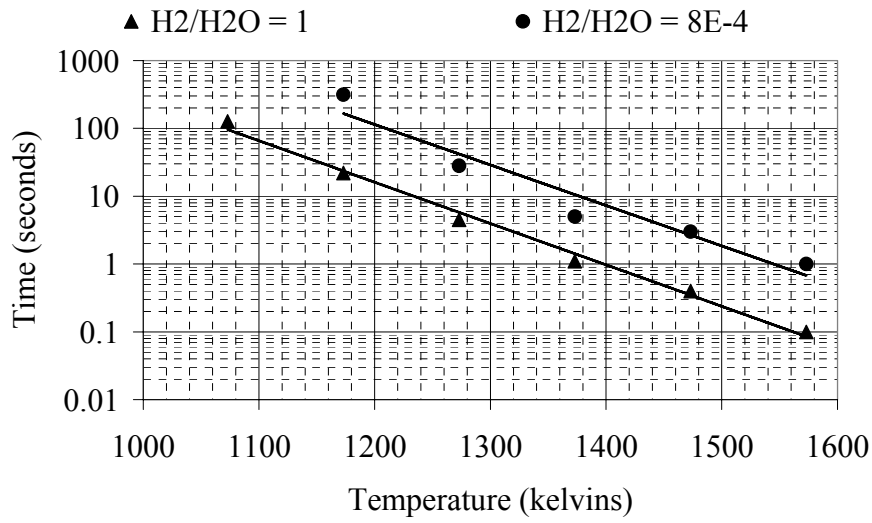


Figure 3: Times to equilibrium for the two H₂/H₂O ratios, as functions of temperature. The times were calculated by the *Zero* program [42].

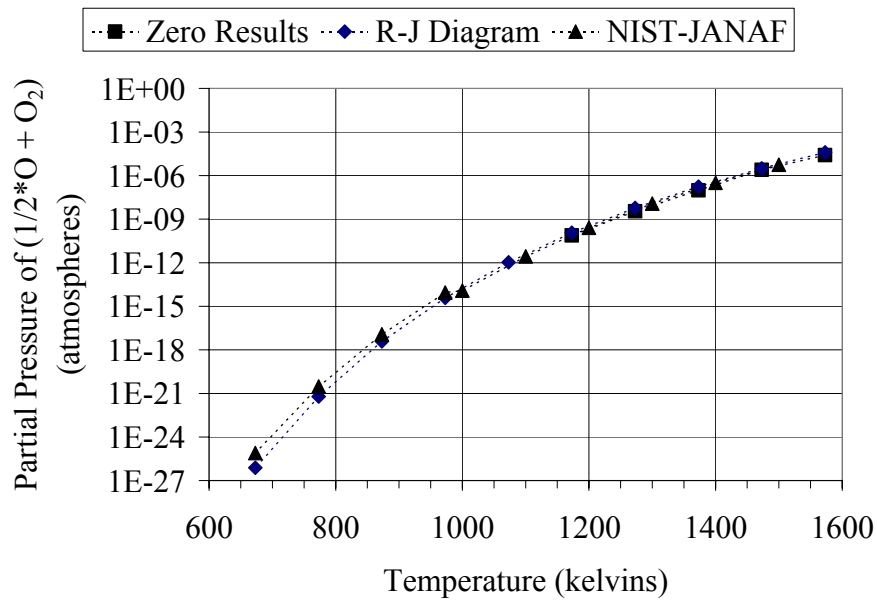


Figure 4: Total equilibrium partial pressure of oxygen as a function of temperature, for a H₂/H₂O ratio of 8·10⁻⁴. For the *Zero* results, the total oxygen is all of the diatomic oxygen plus half of the quantity of monatomic oxygen.

Figure 2 also shows that the $\text{H}_2/\text{H}_2\text{O}$ mechanism equilibrates much faster than the CO/CO_2 mechanism. In fact, the CO/CO_2 ratio of $8 \cdot 10^{-4}$, which represents a value for oxygen control in a practical system, does not even equilibrate in less than 1000 seconds for temperatures below 1473 K (1200°C). This temperature is higher than the maximum operating temperature for many tube furnaces, which would be used to heat the gas mixture. Glassman indicates that if some hydrogen or water vapor is present in the mix—even as little as 20 ppmv—then the CO/CO_2 is catalyzed and reacts much more quickly than highly pure CO and CO_2 [25]. However, no such catalysis was observed in test simulation run on *Zero*. (This result might be due to the fact that the GRI mechanism which was used with *Zero* is calibrated especially for combustion of natural gas.) Even so, intentionally introducing impurities into the CO and CO_2 gases begins to defeat the purpose of precise oxygen control, unless the exact amounts (including lower limits) of the impurities are known and controlled. The conclusion is that the CO/CO_2 system may not be able to control the oxygen content in an LBE system, and in any case, the $\text{H}_2/\text{H}_2\text{O}$ system is certainly a better system for this purpose.

Figure 3 is a plot of the same data for the two cases of the $\text{H}_2/\text{H}_2\text{O}$ system, this time as a function of temperature. This plot is easier for regular use. Again, a linear relationship is seen, between the logarithm of time and the temperature.

Figure 4 compares the *Zero* results for equilibrium oxygen partial pressure with the pressures predicted from the R-J diagram and from the NIST-JANAF tables. It can be seen that all three predictions agree closely, especially above 1000 K. It should be

re-emphasized that a difference of one order of magnitude is quite small due to the logarithmic dependence of the Gibbs free energy on oxygen partial pressure.

The most important result from Figure 2 and Figure 3, however, is that neither the CO/CO₂ system nor even the H₂/H₂O system is capable of reaching equilibrium in a reasonable timeframe at LBE system operating temperatures, around 500°C. In fact, unless a very large furnace is used to heat the gas so that it has a long residence time in which to equilibrate, the minimum temperature at which the gas dynamic equilibrium method can be used is 1000°C (1273 K). This observation—that the H₂/H₂O system is kinetically limited at low temperatures—is corroborated by combustion experiments. For example, the second and fourth figures in the third chapter of Glassman's book show that a stoichiometric mixture of hydrogen and oxygen at one atmosphere of pressure—a more unstable and, therefore, more reactive mixture than the H₂/H₂O mixture used in oxygen control—must be heated above 875 K in order to be explosive [25]. Therefore, the gas dynamic equilibrium method cannot be applied directly, without modification, for oxygen control in LBE systems.

Thankfully, two other physical-chemical processes rescue the gas dynamic equilibrium method for use in oxygen control. First, the equilibrium Gibbs free energy of oxide formation does not change rapidly with temperature, for a given H₂/H₂O ratio. Second, the container surfaces and the even the LBE surface itself can catalyze oxidation reactions to cause them to occur at temperatures lower than those at which they would occur in the gas phase alone.

The R-J diagram is a perfect tool for seeing the first point: that the equilibrium Gibbs free energy of oxide formation does not change rapidly with temperature, for a given H₂/H₂O ratio. In other words, the equilibrium Gibbs free energy—that is, the quantity $(RT \ln p_{O_2})$ —for the reaction



does not vary greatly with temperature. This fact means that a H₂/H₂O mixture which is heated slightly above 1000°C (1273 K) and allowed to equilibrate will not be far from equilibrium when it is cooled back down to an LBE operating temperature around 500°C (773 K). Such a gas mixture will have too much oxygen at the lower temperature (500°C), but this excess oxygen will not have a dramatic effect as long as the target oxygen level is not too close to the oxidation line of a particular metal of interest. Note that although the actual equilibrium oxygen partial pressure may vary over a few orders of magnitude with a temperature change of several hundred degrees Celsius, the logarithmic dependence of the Gibbs free energy on oxygen—that is, $(RT \ln p_{O_2})$ —means that this Gibbs free energy does not change very much.

The second point—that solid or liquid surfaces can catalyze reactions to occur at lower temperatures than those at which they would occur in the gas phase alone—is also borne out by experience. That hydrogen can scavenge oxygen and reduce lead oxide at temperatures lower than 873 K is well established [44-46]. What remains unclear is (1) whether or not the surface-catalyzed reactions reach equilibrium at the same rate as the gas phase reactions and (2) whether or not some differences in the kinetics of the

reactions between lead and hydrogen, oxygen, and water cause a pseudo-equilibrium that is different from the gas phase equilibrium. If the surface-catalyzed reactions are too slow, the H_2/H_2O mixture will not equilibrate during its residence time in contact with the LBE. In this case, the LBE is reacting with a gas with unknown oxygen concentration—a concentration which may be much higher than desired, since the oxygen impurities and leaks would not have been removed through reaction with the hydrogen. Also, if the kinetics of the lead-hydrogen reaction is much slower than the kinetics of the lead-oxygen reaction, for example, then more oxygen will be added to the LBE than would be expected from knowledge of the thermodynamic equilibrium. This situation is the most likely scenario: lead forms oxides readily but not hydrides [47], so if a lead atom pulls apart a water molecule, for example, the oxygen atom will tend to stick with the lead while the hydrogen atoms fly away into the rest of the gas. This might be the cause of an observation by at least two researchers that bubbling H_2/H_2O gas through LBE causes much oxide formation—more than would be expected from the R-J diagram [21, 48]. In any case, the fact is that, although work is being done in the field of surface catalysis [49], surface-catalyzed reactions are not yet completely understood and characterized. Therefore, although one is forced to rely upon them to establish equilibrium between the cover gas and the LBE, they should not be relied upon to establish equilibrium amongst the constituent gases of the gas phase (i.e., equilibrium among hydrogen, oxygen, and water).

It may be curious to the reader as to why many researchers are using the H_2/H_2O gas dynamic equilibrium method—without the pre-heating above 1000°C as mentioned

above—to control the oxygen content of LBE at low temperatures, at which the gas-phase kinetics are so poor as to render the method unreliable. The author’s hypothesis is that the method has been misappropriated from earlier experiments on other systems at higher temperatures. According to Chang, Fitzner, and Zhang [7], the gas dynamic equilibrium method was “pioneered by Chipman and co-workers at MIT for carrying out thermochemical investigations of steelmaking reactions.” Indeed, Chipman and Dastur’s paper entitled, “Equilibrium in the Reaction of Hydrogen with Oxygen in Liquid Iron,” published in 1949 in *Metals Transactions*, is a description of his application of the method to liquid iron [50]. Iron melts 1538°C [47], so Chipman’s experiments (in this paper) were conducted over the temperature range from 1563 to 1750°C. Clearly, these temperatures are well above 873 K, so the H₂/H₂O gas mixture reaches equilibrium extremely quickly. However, when the Russians revealed their LBE technology to the rest of the world in the 1990s, they did not address the kinetics issues in their papers about H₂/H₂O gas dynamic equilibrium oxygen control [31-34]. The first Western paper published on this topic in the *Journal of Nuclear Materials* after this time referenced these Russian authors [30] and also neglected the kinetics. The oversight has propagated throughout the literature since then.

4.2.2. Dilution of Reactive Gases

Since hydrogen can be explosive when mixed with air, it is common to dilute it with a non-reactive gas such as argon in order to reduce its partial pressure to a safe level. For hydrogen gas emitted into the atmosphere, the lower flammability limit is 4% [51], and a safety factor of four reduces this level to 1%. When the hydrogen is diluted, it is the partial, not total, pressure which is used in the calculation of the proper H₂/H₂O ratio in

the product mixture. Commercially bottled gases are usually diluted on a volume, not weight, basis. Since the gases behave almost ideally at room temperature, the volume fraction of a reactive gas in a bottle corresponds to its mole fraction and to its partial pressure, according to the ideal gas law. Thus, a 1% hydrogen / balance argon bottle at 200 kPa contains 1% hydrogen by mole fraction, and the partial pressure of hydrogen is 2 kPa. This relation is very helpful when mixing two diluted gases, since the partial pressure of each of the reactive gases is simply the product of the total pressure of its gas stream and its volume fraction. For example, a gas stream of 1% H₂ (balance argon) mixed at an equal flow rate with a second argon gas stream containing 0.1% (1000 ppmv) H₂O would yield a H₂/H₂O ratio of ten (10.0). Neglecting impurities in the bottled gases, this value could be used directly with the R-J diagram to find the corresponding oxygen partial pressure of the product mixture at its temperature and at thermodynamic equilibrium.

In contrast with hydrogen, carbon monoxide cannot be diluted to make it safe, because it is its toxicity—not its explosiveness—which is usually the major risk to human health and safety. According to the *NIOSH Pocket Guide to Chemical Hazards* [52], the lower explosion limit of carbon monoxide is 12.5%, but the NIOSH Recommended Exposure Limit is only 35 ppm, the OSHA Permissible Exposure Limit is 50 ppm, the NIOSH Ceiling value is 200 ppm, and the air concentration which is “Immediately Dangerous to Life and Health” is 1200 ppm (0.12%). These limits are due to the asphyxiating property of carbon monoxide: the carbon monoxide displaces the oxygen in the bloodstream [53]. Theoretically, one could dilute the CO with argon down to 35 ppm or less, but doing so

would make the gas practically useless, as will be explained later in the section on swamping leaks and gas impurities.

4.2.3. Configuration of a Hydrogen-Water Oxygen Control System

For experimental investigations into LBE corrosion, it would be ideal to be able to vary the oxygen content over a wide range: from the level where oxidation of the least reactive metal occurs to the level where the most stable oxide of interest decomposes. According to Table 1, the least reactive metal is bismuth. However, in a lead-bismuth alloy such as LBE, the lead will have to oxidize almost completely before the bismuth begins to oxidize, but by then this lead oxide would have completely fouled and even plugged the piping system. Therefore, from a practical standpoint, the least reactive metal is the lead. For stainless steels the most stable oxide of interest is probably chromium oxide, which is the most stable oxide of the major constituent alloying metals in the steels. This range—from oxidation of lead to the decomposition of chromium oxide—corresponds at 500°C to a range of oxygen partial pressures from $1 \cdot 10^{-17}$ atmospheres to $1 \cdot 10^{-42}$ atmospheres and to a range of H_2/H_2O ratios from $1 \cdot 10^{-5}$ to $1 \cdot 10^7$, respectively, according to the R-J diagram. Thus, the H_2/H_2O gas dynamic equilibrium method must control the oxygen content over a range of 25 orders of magnitude via setting the H_2/H_2O ratio over a range of 12 orders of magnitude.

Unfortunately, practical systems employing the H_2/H_2O gas dynamic equilibrium method cannot cover this entire range. The lowest controllable H_2/H_2O ratio which is attainable is about $1 \cdot 10^{-4}$, if pure steam and 1% H_2 /balance Ar gas are used. Due to impurities even in research-grade gases, the highest H_2/H_2O ratio is about $1 \cdot 10^3$, if 1% H_2 /balance Ar gas

is used, or about $1 \cdot 10^5$, if pure H_2 gas is used. However, if the laboratory is not equipped with hydrogen safety enclosures and equipment, the 1% H_2 /balance Ar gas must be used. (See the section on dilution of reactive gases.) At $500^\circ C$, these lowest and highest ratios correspond approximately to $1 \cdot 10^{-19}$ atmospheres and $1 \cdot 10^{-33}$ atmospheres of oxygen, respectively. At $1 \cdot 10^{-19}$ atmospheres of oxygen, lead just barely begins to oxidize; at $1 \cdot 10^{-33}$ atmospheres of oxygen, any iron oxide on the steel will decompose, but any chromium oxide will not.

Though this limited range of oxygen control is not ideal, it does cover the important range between the start of the oxidation of the stainless steel and the start of the oxidation of the lead; this is the range in which practical, large-scale LBE systems would likely operate. Also, the upper limit of oxygen content is not so important because the LBE experiments can be carried out in an air atmosphere in order to cause the lead to oxidize. Lastly, the lower limit is beneath the oxidation line for iron, so the iron-chromium spinel, which is often the protective oxide layer found on stainless steel samples that are immersed in LBE, will decompose (possibly to pure chromium oxide). Therefore, many meaningful experiments can be carried out using the limited range of oxygen control that the H_2/H_2O gas dynamic equilibrium method provides.

Depending on the oxygen content desired, the H_2/H_2O gas system must be reconfigured to provide the proper control. There are three basic configurations:

- 1) a stream of 1% H_2 and a stream of steam
- 2) a stream of 1% H_2 and a stream of humidified argon

3) a stream of humidified 1% H₂

The argon and the hydrogen can be humidified either at the bottling plant by the gas supplier or by passing the argon through humidification equipment. However, the maximum amount of water that Matheson Tri-Gas will provide in certified argon is 150 ppmv [54]; and in the case of bottled humidified hydrogen, a separate bottle would have to be purchased for each H₂/H₂O ratio desired. Using some sort of humidification scheme in the laboratory provides much more flexibility in the amount of water to be added to the gas streams; however, it also introduces more impurity, namely oxygen. Table 3 shows which H₂/H₂O ratios the various humidification methods can provide, assuming research-grade argon and hydrogen (99.9999% pure).

Table 3: Achievable H₂/H₂O ratios with various methods of adding water vapor to 1% H₂, balance Ar

H ₂ / H ₂ O							
10 ⁻⁴	10 ⁻³	10 ⁻²	10 ⁻¹	10 ⁰	10 ¹	10 ²	10 ³
Steam							
		10,000 ppmv H ₂ O added to pure Ar					
		1000 ppmv H ₂ O added to pure Ar					
		100 ppmv H ₂ O added to pure Ar					
		Bottled (Ar + 100 ppmv H ₂ O)					
		H ₂ O added directly to 1% H ₂ , balance Ar					
				10000 ppmv	1000 ppmv	100 ppmv	None

Once a humidification scheme has been chosen for a particular experiment (for example, 1000 ppmv added to Ar), the flexibility in the H₂/H₂O ratio can be achieved by using high-precision, gas mass-flow controllers to proportion the gas flows. Thus, for example, 1000 mL/min of an Ar gas stream that has been humidified to 1000 ppmv H₂O can be mixed with 10 mL/min of a 1% H₂ gas stream to create a final gas stream with a H₂/H₂O ratio of 1·10⁻¹. The amount of proportioning available using gas mass-flow controllers is limited to approximately two orders of magnitude because of two considerations. First, the maximum amount of gas flow permissible in a bench-top laboratory setup is about 1000 mL/min. If the flowrate is much greater than this value, too much high-purity gas is used, and the cost rises dramatically. Also, since argon displaces oxygen in the atmosphere and in sufficient quantity could cause asphyxia, high flowrates would require that a dedicated, high-flow ventilation system be installed in the laboratory. In addition, if the gas is being injected below the surface of the liquid LBE and bubbled through the LBE, flowrates much greater than 1000 mL/min cause excessive turbulence in the retort: the LBE splashes everywhere. Second, the minimum amount of gas flow permissible is about 10 mL/min, because of concerns about leaks in the gas piping system. This consideration will be explained in more detail below.

It should be pointed out that a typical accuracy on high-precision, gas mass-flow controllers is about 1% of full scale [55]. For example, a controller rated for 1000 mL/min would have an accuracy of ±10 mL/min. Therefore, this controller should not be used to control a gas flow at a target value of 10 mL/min, because approximately 100% error would result. It may be feasible, though, to use a 100 mL/min controller on a 10

mL/min stream, or to use a 1000 mL/min controller on a 100 mL/min stream. The feasibility will depend on the purity of the streams—whether or not the research can tolerate the additional error introduced by imprecise gas metering. An error analysis should be conducted on the gas system to determine the impact of this level of accuracy.

4.2.4. Swamping of Leaks and Impurities

One of the chief concerns that initially confront researchers attempting to construct an oxygen control system is the issue of gas impurities and leaks in the gas piping. Since the target oxygen levels are much lower than those of the purest of available gases, it is often initially assumed that extremely stringent gas purification must be undertaken and also that any level of leaking in the piping system is unacceptable because of the introduction of oxygen from the air into the piping. Recall that, according to Dalton's law of partial pressures, each type of gas in a mixture behaves as though it was the only gas in the environment. Therefore, the oxygen in the air sees an almost complete vacuum in the piping system and will quickly rush into the system through any available opening, regardless of the fact that the total pressure in the system is greater than atmospheric pressure and, therefore, gas is actually leaking out of the system. If these concerns about purity and leaking were unable to be addressed, the gas dynamic equilibrium method would be completely unfeasible because the error introduced by the impurities and leaks would overwhelm any control achieved by the method.

Fortunately and perhaps obviously, the gas dynamic equilibrium method itself inherently mitigates these concerns. The whole point of the method is to use a chemical balance of macroscopic (that is, meter-able) levels of gases to control the quantity of a microscopic

(that is, un-meter-able) level of gas (that is, oxygen). This fact means that as long as the quantities of hydrogen and water are much, much greater than the levels of impurities and leakage, the effects of the impurities and leakage are completely swamped by the effects of the reaction between the hydrogen and the water. This fact does not mean, however, that a researcher can be careless about impurities and leakage; an error analysis should be performed to see the effects of certain levels of impurities and/or leakage. Impurities are of primary importance, because it is impossible to use an excessively impure gas to swamp its own impurities!

An analysis of the errors introduced by impurities is relatively straightforward. Let X denote the flow of pure argon; let Y denote the flow of 1% H_2 , balance Ar; let v denote the concentration of water to be added to one or the other of the gas streams; and let Z denote the resulting flow of water vapor (mixed in with the argon or directly with the hydrogen). Let subscripts denote the level of the particular impurities in the gas stream of the variable; for example, X_{O_2} would indicate the mole fraction of oxygen impurity in the “pure” argon stream. Note that Z_{O_2} denotes the oxygen dissolved in the water, which is assumed to volatilize to the same concentration as its dissolved concentration. For simplicity, assume that the carbon dioxide, carbon monoxide, and hydrocarbon impurities approximately balance each other out. Then, the major impurities of concern are water vapor and oxygen. Lastly, for the calculation of the actual H_2/H_2O ratio, assume that all of the oxygen impurity is reacted with the hydrogen to form water vapor. Once the H_2/H_2O ratio has been calculated, the R-J diagram will tell what the final equilibrium partial pressure of the oxygen actually is.

With the above considerations, the ideal (no impurities) and actual (with impurities) H_2/H_2O ratios can be calculated as follows. First are the equations for the case when the water vapor is added to pure argon, which is subsequently mixed with the 1% hydrogen:

$$\left. \frac{H_2}{H_2O} \right|_{\text{ideal}} = \frac{0.01 \cdot Y}{vX} = \frac{0.01 \cdot Y}{Z} \quad \text{Equation 37}$$

$$\left. \frac{H_2}{H_2O} \right|_{\text{actual}} = \frac{(0.01 \cdot Y) - 2 \cdot (X_{O_2} + Y_{O_2} + Z_{O_2})}{Z + (X_{H_2O} + Y_{H_2O}) + 2 \cdot (X_{O_2} + Y_{O_2} + Z_{O_2})} \quad \text{Equation 38}$$

Next are the equations for the case when the water vapor is added directly to the 1% hydrogen, either through humidification or through mixing with “pure” steam:

$$\left. \frac{H_2}{H_2O} \right|_{\text{ideal}} = \frac{0.01 \cdot Y}{vY} = \frac{0.01 \cdot Y}{Z} \quad \text{Equation 39}$$

$$\left. \frac{H_2}{H_2O} \right|_{\text{actual}} = \frac{(0.01 \cdot Y) - 2 \cdot (Y_{O_2} + Z_{O_2})}{Z + (Y_{H_2O}) + 2 \cdot (Y_{O_2} + Z_{O_2})} \quad \text{Equation 40}$$

An example of an error analysis is given in Table 4.

Two aspects of these equations are noteworthy. First, the oxygen impurity removes twice its concentration in hydrogen, while simultaneously adding the same amount to the water content, according to the reaction in Equation 19:



(One might be tempted to try to use a controlled amount of oxygen impurity mixed with hydrogen to achieve a certain final oxygen concentration. Closer inspection, though, reveals that the difference in the numerators of Equation 38 and Equation 40 causes excessive sensitivity to impurity oxygen levels and thereby makes fine control of oxygen

content impossible.) For this reason, it is important to reduce the oxygen impurity levels to be as low as possible. This reduction can be achieved by purchasing high-purity gases and by deaerating the water used for humidification, since as much as $2.3 \cdot 10^{-5}$ mole fraction of oxygen is soluble in water at 25°C [47]. (Note that this mole fraction can be directly converted to ppmv only after the water has turned to vapor, since the ideal gas law does not apply to liquid water). Since the solubility of oxygen in water decreases with increasing temperature, deaeration of the water can be accomplished by bringing the water to a boil, to squeeze out the oxygen, and then cooling the water, preferably without contacting it with air to avoid re-oxygenating it. Second, the addition of the water vapor directly to the hydrogen gas stream results in less error, because the impurities of the “pure” argon are not included. Therefore, the steam system and the system of direct humidification of the hydrogen are the best systems for reducing impurity levels in the final gas stream.

Regarding leaks in the piping system, they can be mostly ignored as long as they are not large. With a CO/CO₂ system and a concentration of CO of about 35 ppmv (for safety), even a small leak of air will lead to excess oxygen of about that level, rendering the CO/CO₂ system useless for oxygen control. With a H₂/H₂O system, on the other hand, using a leak-detecting solution such as Snoop® to eliminate the detectable leaks is probably sufficient. The goal is to reduce the amount of oxygen leaking into the piping system to below 1 mL/min. At the lowest hydrogen flowrate of 10 mL/min, a leak of 1 mL/min would introduce an error of about 60%; remember that the oxygen consumes hydrogen to make water, thus amplifying the error beyond that caused by dilution with

water alone. This error is less than an order of magnitude, and for most practical oxygen control situations, such a level of accuracy is sufficient. It is for this reason that the lowest flowrates should be no lower than 10 mL/min, so that the leaks can be sufficiently swamped and ignored.

Table 4: Example of an error analysis of the impurities in a system of a gas stream of 1% H₂, balance Ar, mixed with a gas stream of humidified “pure” Ar. Symbols are as defined in the text.

Research-Grade Impurity Levels [5]		
X _{O2} =	3	ppmv O ₂
Y _{O2} =	2	ppmv O ₂
Z _{O2} =	23	ppmv O ₂
X _{H2O} =	5	ppmv H ₂ O
Y _{H2O} =	3	ppmv H ₂ O

X (mL/ min)	Y (mL/ min)	v (ppmv H ₂ O)	Z (mL/ min)	H ₂ /H ₂ O (ideal)	H ₂ /H ₂ O (actual)	error (absolute)	error (relative)
10	1000	100	0.001	1.E+04	1.2E+03	-8.8E+03	-88%
10	100	100	0.001	1.E+03	5.7E+02	-4.3E+02	-43%
10	10	100	0.001	1.E+02	8.8E+01	-1.2E+01	-12%
100	10	100	0.010	1.E+01	9.3E+00	-6.9E-01	-7%
1000	10	100	0.100	1.E+00	8.9E-01	-1.1E-01	-11%
10	1000	1000	0.010	1.E+03	5.9E+02	-4.1E+02	-41%
10	100	1000	0.010	1.E+02	9.3E+01	-7.1E+00	-7%
10	10	1000	0.010	1.E+01	9.9E+00	-1.4E-01	-1%
100	10	1000	0.100	1.E+00	9.9E-01	-1.3E-02	-1%
1000	10	1000	1.000	1.E-01	9.3E-02	-6.7E-03	-7%
10	1000	10000	0.100	1.E+02	9.3E+01	-6.6E+00	-7%
10	100	10000	0.100	1.E+01	9.9E+00	-8.0E-02	-1%
10	10	10000	0.100	1.E+00	1.0E+00	-2.4E-03	0%
100	10	10000	1.000	1.E-01	9.9E-02	-7.6E-04	-1%
1000	10	10000	10.000	1.E-02	9.3E-03	-6.6E-04	-7%

The last and perhaps most remarkable conclusion from error analyses of H₂/H₂O oxygen control systems is that the incoming gas does not need to be pre-treated in the laboratory to remove impurities before being used, as long as the initial purity of the gas is sufficiently high. As Table 4 demonstrates, the impurities in research-grade (99.9999% purity) argon and 1%-hydrogen/argon mixed gases do not cause significant errors. It is even questionable whether using pre-treatments such as hot copper or titanium chips or lithium-hydride tubes helps or actually hinders gas purity for research-grade gases, since the additional tubing and joints adds more potential for leaks to develop. The tradition of pre-treating the gases originated at least as far back as the 1940s, when John Chipman at MIT was using the gas dynamic equilibrium method to control the oxygen content in molten iron [50, 56]. On page 172 of the paper he coauthored with Gokcen, he mentions that the argon that he used was commercial argon of welding or lamp grade. Today's commercial grade argon has a purity of only 99.95% [57]—that is, there is 500 ppmv of unknown impurities in this grade of gas—and it is likely that the purity of gas in the 1940s was even worse. Therefore, pre-treating the gas to remove most of these impurities was important in those days, to reduce errors in the experiment. With the availability of today's ultra-high-purity and research-grade gases, however, such pre-treatment is unnecessary for use in the gas dynamic equilibrium method of oxygen control.

5. Conclusion

Measurement and control of the oxygen content of the cover gas in an LBE system is critical to controlling the corrosion of the materials in the system. From this study, the YSZ solid-electrolyte oxygen sensor is the sensor of choice for the high temperatures and low oxygen partial pressures of these systems. For controlling the oxygen partial pressure, gas purification schemes are futile, because the target partial pressures are well below those achievable even with the best purification technologies. Instead, the gas dynamic equilibrium method—specifically the $\text{H}_2/\text{O}_2/\text{H}_2\text{O}$ system—is the most promising method for control of large, full-scale LBE systems. Use of this method, however, requires consideration of the kinetics of the gas-phase reactions, because at operating temperatures of LBE systems (around 500°C), these gases do not react with each other, except by surface catalysis. Therefore, preheating the gas mixture to above 1000°C and allowing it to equilibrate before introducing it to the LBE system is an essential experimental step. Also, an error analysis of the gas system—considering both leaks and impurities—is important (1) to ensure that the gas system is producing the desired oxygen content and (2) so that extra costs can be avoided by avoiding unnecessary purification measures. Other details for configuration of a gas dynamic equilibrium system have also been given.

6. Recommendations for Future Work

This thesis has focused on the control of the oxygen content of the cover gas of an LBE system. However, the other major component of the total oxygen control theory is what happens in the liquid phase: the dissolving of oxygen into the liquid LBE, its transport—whether by diffusion or convection—to steel surfaces, and its reaction with the steel constituent elements. Some work has already been done in these areas. For example, Zhang and Li have written about LBE corrosion kinetics [58, 59]. Also, Ganesan, et al., have written about diffusion, activity, and solubility of oxygen in LBE [15]. However, more work can still be done in these areas.

Another important topic for evaluation is the reliability and kinetics of zirconia-based oxygen sensors, for use both in the gas phase and in the liquid LBE directly. At the relatively low operating temperatures of LBE systems (around 500°C), the kinetics of the reactions in YSZ sensors are not very good. This area needs to be explored further.

Appendix

Table 5: Kinetic rate constants and equilibrium constants for reactions in the H₂/O₂/H₂O and CO/O₂/CO₂ mechanisms. The reactions are from *Combustion* [25] and the data are calculated from *Combustion* and the NIST-JANAF tables [41]. See Table 2 for the units of the rate constants. Equilibrium constants are unitless.

Reaction	k _{forward}	K _{pf@ 1373 K}	k _{backward}
H + O ₂ ⇌ O + OH	4.69E+11	3.81E-02	1.23E+13
O + H ₂ ⇌ H + OH	1.21E+12	1.12E+00	1.08E+12
OH + H ₂ ⇌ H + H ₂ O	3.36E+12	5.47E+01	6.14E+10
O + H ₂ O ⇌ OH + OH	4.73E+10	1.98E-01	2.39E+11
H ₂ + Ar ⇌ H + H + Ar	5.06E-02	6.52E-06	7.76E+03
O + O + Ar ⇌ O ₂ + Ar	3.68E+13	8.31E+05	4.43E+07
H + OH + Ar ⇌ H ₂ O + Ar	4.41E+15	5.14E+12	8.58E+02
H + O ₂ + Ar ⇌ HO ₂ + Ar	2.18E+15	1.05E+03	2.08E+12
H + O ₂ ⇌ HO ₂	4.52E+13	1.05E+03	4.32E+10
HO ₂ + H ⇌ H ₂ + O ₂	3.03E+13	8.99E+07	3.37E+05
HO ₂ + H ⇌ OH + OH	1.23E+14	3.71E+07	3.31E+06
HO ₂ + O ⇌ OH + O ₂	2.03E+13	1.01E+08	2.01E+05
HO ₂ + OH ⇌ H ₂ O + O ₂	1.38E+13	4.92E+09	2.81E+03
HO ₂ + HO ₂ ⇌ H ₂ O ₂ + O ₂	5.44E+12	4.65E+01	1.17E+11
H ₂ O ₂ + Ar ⇌ OH + OH + Ar	2.73E+09	1.30E+00	2.10E+09

Table 5, continued

Reaction	k_{forward}	$K_{\text{pf @ 1373 K}}$	k_{backward}
$\text{H}_2\text{O}_2 \Leftrightarrow \text{OH} + \text{OH}$	5.93E+06	1.30E+00	4.55E+06
$\text{H}_2\text{O}_2 + \text{H} \Leftrightarrow \text{H}_2\text{O} + \text{OH}$	2.68E+12	6.91E+11	3.88E+00
$\text{H}_2\text{O}_2 + \text{H} \Leftrightarrow \text{H}_2 + \text{HO}_2$	2.62E+12	3.30E+03	7.94E+08
$\text{H}_2\text{O}_2 + \text{O} \Leftrightarrow \text{OH} + \text{HO}_2$	4.24E+12	3.69E+03	1.15E+09
$\text{H}_2\text{O}_2 + \text{OH} \Leftrightarrow \text{H}_2\text{O} + \text{HO}_2$	1.84E+13	1.80E+05	1.02E+08
$\text{CO} + \text{O} + \text{Ar} \Leftrightarrow \text{CO}_2 + \text{Ar}$	1.16E+14	2.81E+12	4.12E+01
$\text{CO} + \text{O}_2 \Leftrightarrow \text{CO}_2 + \text{O}$	6.49E+05	1.02E+00	6.38E+05
$\text{CO} + \text{OH} \Leftrightarrow \text{CO}_2 + \text{H}$	2.38E+11	2.67E+01	8.91E+09
$\text{CO} + \text{HO}_2 \Leftrightarrow \text{CO}_2 + \text{OH}$	1.34E+10	1.02E+08	1.31E+02

References

- [1] G.V. Samsonov (Ed.), The Oxide Handbook, (1982).
- [2] F.D. Richardson and J.H.E. Jeffes, The Thermodynamics of Substances of Interest in Iron and Steel Making from 0°C to 2400°C, Journal of the Iron and Steel Institute, 160 (1948) 261-270.
- [3] H.J.T. Ellingham, Journal of the Society of Chemical Industry, 63 (1944) 125.
- [4] L.S. Darken, R.W. Gurry and M.B. Bever, Physical Chemistry of Metals, McGraw-Hill, New York, 1953.
- [5] Matheson Tri-Gas Sales Literature, (2006).
- [6] N. Li, Active Control of Oxygen in Molten Lead-Bismuth Eutectic Systems to Prevent Steel Corrosion and Coolant Contamination, Journal of Nuclear Materials, 300 (2002) 73-81.
- [7] Y.A. Chang, K. Fitzner and M.X. Zhang, The Solubility of Gases in Liquid Metals and Alloys, Progress in Materials Science, 32 (1988) 97-259.
- [8] Orbisphere Sales Literature, www.orbisphere.com, (2006).
- [9] Ocean Optics Sales Literature, www.oceanoptics.com, (2006).
- [10] Cambridge Sensotec Sales Literature, www.cambridge-sensotec.co.uk, (2006).
- [11] K.L. Komarek, Experimental Techniques in High Temperature Thermodynamics, Pure and Applied Chemistry, 64 (1992) 93-102.
- [12] J.W. Patterson, Conduction Domains for Solid Electrolytes, Journal of the Electrochemical Society, 118 (1971) 1033-1039.
- [13] A.J. Moulson and J.M. Herbert, Electroceramics: Materials, Properties, Applications, Chapman & Hall, London, 1990.
- [14] R. Ganesan, T. Gnanasekaran and R.S. Srinivasa, Standard Molar Gibbs Free Energy of Formation of PbO(s) Over a Wide Temperature Range from EMF Measurements, Journal of Nuclear Materials, 320 (2003) 258-264.
- [15] R. Ganesan, T. Gnanasekaran and R.S. Srinivasa, Diffusivity, Activity and Solubility of Oxygen in Liquid Lead and Lead-Bismuth Eutectic Alloy by Electrochemical Methods, Journal of Nuclear Materials, 349 (2006) 133-149.

- [16] J. Konys, H. Muscher, Z. Voß and O. Wedemeyer, Oxygen Measurements in Stagnant Lead–Bismuth Eutectic Using Electrochemical Sensors, *Journal of Nuclear Materials*, 335 (2004) 249-253.
- [17] J.L. Courouau, Electrochemical Oxygen Sensors for On-Line Monitoring in Lead–Bismuth Alloys: Status of Development, *Journal of Nuclear Materials*, 335 (2004) 254-259.
- [18] J.A. Fernández, J. Abellà, B. J. and L. Victori, Development of an Oxygen Sensor for Molten 44.5% Lead–55.5% Bismuth Alloy, *Journal of Nuclear Materials*, 301 (2002) 47-52.
- [19] J. Konys, H. Muscher, Z. Voß and O. Wedemeyer, Development of Oxygen Meters for the Use in Lead-Bismuth, *Journal of Nuclear Materials*, 296 (2001) 289-294.
- [20] V.A. Blochin, E.G. Budylov, R.I. Velikanovitch, I.N. Gorelov, A.N. Deryugin, Z.I. Ievleva, M.I. Kozina, Y.A. Musihin, I.D. Ponimash, A.D. Sorokin, A.L. Shimkevich, B.A. Shmatko and E.G. Shcherbakov, Experience of Development and Operation of Oxide Electrolytic Sensors in Lead-Bismuth Coolants, *Heavy Liquid Metal Coolants in Nuclear Technology*, Obninsk, Russia October 5-9, 1998 2 2 (1999) 588-592.
- [21] J.L. Courouau, P. Trabuc, G. Laplanche, P. Deloffre, P. Taraud, M. Ollivier, R. Adriano and S. Trambaud, Impurities and Oxygen Control in Lead Alloys, *Journal of Nuclear Materials*, 301 (2002) 53-59.
- [22] V. Ghetta, F. Gamaoun, J. Fouletier, M. Hénault and A. Lemoulec, Experimental Setup for Steel Corrosion Characterization in Lead Bath, *Journal of Nuclear Materials*, 296 (2001) 295-300.
- [23] A.L. Johnson, D. Parsons, J. Manzerova, D.L. Perry, D. Koury, B. Hosterman and J.W. Farley, Spectroscopic and Microscopic Investigation of the Corrosion of 316/316L Stainless Steel by Lead–Bismuth Eutectic (LBE) at Elevated Temperatures: Importance of Surface Preparation, *Journal of Nuclear Materials*, 328 (2004) 88-96.
- [24] M.W. Chase Jr., C.A. Davies, J.R. Davies, D.J. Fulrip, R.A. McDonald and A.N. Syverud (Ed.), *JANAF Thermochemical Tables*, *Journal of Physical and Chemical Reference Data*, Vol. 14, Supplement 1, (1985).
- [25] I. Glassman, *Combustion*, Academic Press, San Diego, 1996.
- [26] M. Kondo, M. Takahashi, T. Suzuki, K. Ishikawa, K. Hata, Q. Suizheng and H. Sekimoto, Metallurgical Study on Erosion and Corrosion Behaviors of Steels Exposed to Liquid Lead–Bismuth Flow, *Journal of Nuclear Materials*, 343 (2005) 349-359.

- [27] D. Gómez Briceño, L. Soler Crespo, F.J. Martín Muñoz and F. Hernández Arroyo, Influence of Temperature on the Oxidation/Corrosion Process of F82Hmod. Martensitic Steel in Lead–Bismuth, *Journal of Nuclear Materials*, 303 (2002) 137-146.
- [28] L. Soler Crespo, F.J. Martín Muñoz and D. Gómez Briceño, Short-Term Static Corrosion Tests in Lead-Bismuth, *Journal of Nuclear Materials*, 296 (2001) 273-281.
- [29] C. Lefhalm, J.U. Knebel and K.J. Mack, Kinetics of Gas Phase Oxygen Control System (OCS) for Stagnant and Flowing Pb-Bi Systems, *Journal of Nuclear Materials*, 296 (2001) 301-304.
- [30] G. Müller, G. Schumacher and F. Zimmermann, Investigation on Oxygen Controlled Liquid Lead Corrosion of Surface Treated Steels, *Journal of Nuclear Materials*, 278 (2000) 85-95.
- [31] V.A. Gulevsky, P.N. Martynov, Y.I. Orlov and M.E. Chernov, Application of Hydrogen/Water Vapor Mixtures in Heavy Coolant Technology, Heavy Liquid Metal Coolants in Nuclear Technology, Obninsk, Russia October 5-9, 1998 2 (1999) 668-674.
- [32] I.V. Gorynin, G.P. Karpov, V.G. Markov, V.S. Lavrukhin and V.A. Yakovlev, Structural Materials for Power Plants with Heavy Liquid Metals as Coolants, Heavy Liquid Metal Coolants in Nuclear Technology, Obninsk, Russia Oct. 5-9, 1998 2 1 (1999) 120-132.
- [33] B.F. Gromov, Y.I. Orlov, P.N. Martynov and V.A. Gulevsky, The Problems of Technology of the Heavy Liquid Metal Coolants (Lead-Bismuth, Lead), Heavy Liquid Metal Coolants in Nuclear Technology, Obninsk, Russia October 5-9, 1998 2 1 (1999) 87-100.
- [34] B.F. Gromov, Y.I. Orlov, P.N. Martynov, K.D. Ivanov and V.A. Gulevsky, Physical-Chemical Principles of Lead-Bismuth Coolant Technology, in H.U. Borgstedt, F. G. (Eds.), *Liquid Metal Systems: Material Behavior and Physical Chemistry in Liquid Metal Systems 2*, Plenum, New York, 1995, pp. 339-343.
- [35] L. Soler Crespo, F.J. Martín Muñoz, F. Hernández Arroyo and D. Gómez Briceño, Corrosion of Stainless Steels in Lead–Bismuth Eutectic up to 600 °C, *Journal of Nuclear Materials*, 335 (2004) 174-179.
- [36] T. Furukawa, G. Müller, G. Schumacher, A. Weisenburger, A. Heinzl and K. Aoto, Effect of Oxygen Concentration and Temperature on Compatibility of ODS Steel with Liquid, Stagnant Pb45Bi55, *Journal of Nuclear Materials*, 335 (2004) 189-193.

- [37] G. Ilincev, D. Kárník, M. Paulovic and A. Doubková, The Impact of the Composition of Structural Steels on Their Corrosion Stability in Liquid Pb–Bi at 500 and 400 °C with Different Oxygen Concentrations, *Journal of Nuclear Materials*, 335 (2004) 210-216.
- [38] G. Müller, A. Heinzl, G. Schumacher and A. Weisenburger, Control of Oxygen Concentration in Liquid Lead and Lead–Bismuth, *Journal of Nuclear Materials*, 321 (2003) 256-262.
- [39] E.P. Loewen and H. Yount, HT-9 Corrosion Growth in Flowing Pb-Bi at 550 and 650°C, *American Nuclear Society Transactions*, 87 (2002) 372-374.
- [40] J.L. Latham, *Elementary Reaction Kinetics*, Butterworths, London, 1962.
- [41] M.W. Chase Jr. (Ed.), *NIST-JANAF Thermochemical Tables*, *Journal of Physical and Chemical Reference Data*, (1998).
- [42] D.G. Goodwin, *Zero: A Zero-Dimensional Kinetics Simulator*, Pasadena, California, (2001).
- [43] G.P. Smith, D.M. Golden, M. Frenklach, N. Moriarty, B. Eiteneer, M. Goldenberg, C.T. Bowman, R.K. Hanson, S. Song, J. Gardiner, W. C., V.V. Lissianski and Z. Qin, *GRI-MECH 3.0*, Des Plaines, IL, http://www.me.berkeley.edu/gri_mech/ (1999).
- [44] P.N. Martynov and Y.I. Orlov, Slagging Processes in Lead-Bismuth Loop: Prevention and Elimination of Critical Situations, *Heavy Liquid Metal Coolants in Nuclear Technology*, Obninsk, Russia October 5-9, 1998, Vol. 2 of 2 (1999) 565-576.
- [45] J.V. Cathcart and W.D. Manly, A Technique for Corrosion Testing in Liquid Lead, *Corrosion*, 10 (1954) 432-434.
- [46] I. Ricapito, C. Fazio and G. Benamati, Preliminary Studies on PbO Reduction in Liquid Pb–Bi Eutectic by Flowing Hydrogen, *Journal of Nuclear Materials*, 301 (2002) 60-63.
- [47] D.R. Lide (Ed.), *CRC Handbook of Chemistry and Physics*, (1992).
- [48] N. Li, personal communication, Los Alamos, New Mexico, (2005).
- [49] R.J. Kee, M.E. Coltrin and P. Glarborg, *Chemically Reacting Flow: Theory and Practice*, Wiley-Interscience, Hoboken, New Jersey, 2003.
- [50] M.N. Dastur and J. Chipman, Equilibrium in the Reaction of Hydrogen with Oxygen in Liquid Iron, *Metals Transactions*, 185 (1949) 441-445.

- [51] G. Glass, R. Bourque, S. Basquin and R. Ott, Hydrogen Gas Safety: Self-Study, Los Alamos National Laboratory Los Alamos, New Mexico (2003).
- [52] C.D.C. Department of Health and Human Services, National Institute for Occupational Safety and Health, NIOSH Pocket Guide To Chemical Hazards, Department of Health and Human Services, Centers for Disease Control and Prevention, National Institute for Occupational Safety and Health, Cincinnati, Ohio, 2005.
- [53] O.S.H.A. U.S. Department of Labor, OSHA Fact Sheet: Carbon Monoxide Poisoning, (2002) 1-2.
- [54] Matheson Tri-Gas, personal communication.
- [55] Alicat Scientific Sales Literature, <http://www.alicatscientific.com>, (2003).
- [56] N.A. Gokcen and J. Chipman, Silicon-Oxygen Equilibrium in Liquid Iron, Journal of Metals, Transactions AIME, February (1952) 171-181.
- [57] S. J. Smith Welding Supply, personal communication, Urbana, IL, (2006).
- [58] J. Zhang and N. Li, Corrosion/Precipitation in Non-Isothermal and Multi-Modular LBE Loop Systems, Journal of Nuclear Materials, 326 (2004) 201-210.
- [59] J. Zhang and N. Li, A Correlation for Steel Corrosion in Non-Isothermal LBE Loops, Journal of Nuclear Science and Technology, 41 (2004) 260-264.